**REPUBLIC OF TURKEY**
**YILDIZ TECHNICAL UNIVERSITY**
**GRADUATE SCHOOL OF SCIENCE AND ENGINEERING**

# DEVELOPMENT OF DECISION MAKING MECHANISM FOR ENERGY TRANSITION BETWEEN ELECTRIC VEHICLES IN PARKING LOTS CONSIDERING VEHICLE TO VEHICLE

**Hilmi Cihan GÜLDORUM**

MASTER OF SCIENCE THESIS
Department of Electrical Engineering
Program of Electrical Power Systems

Advisor
Assoc. Prof. Ozan ERDİNÇ

Co-Advisor
Asst. Prof. İbrahim ŞENGÖR

July, 2021

**REPUBLIC OF TURKEY**
**YILDIZ TECHNICAL UNIVERSITY**
**GRADUATE SCHOOL OF SCIENCE AND ENGINEERING**

# DEVELOPMENT OF DECISION MAKING MECHANISM FOR ENERGY TRANSITION BETWEEN ELECTRIC VEHICLES IN PARKING LOTS CONSIDERING VEHICLE TO VEHICLE

A thesis submitted by Hilmi Cihan GÜLDORUM in partial fulfillment of the requirements for the degree of **MASTER OF SCIENCE** is approved by the committee on 01.07.2021 in Department of Electrical Engineering, Program of Electrical Power Systems.

Assoc. Prof. Ozan ERDİNÇ
Yıldız Technical University
Advisor

Asst. Prof. İbrahim ŞENGÖR
Izmir Kâtip Celebi University
Co-Advisor

**Approved By the Examining Committee**

Assoc. Prof. Ozan ERDİNÇ, Advisor
Yıldız Technical University _____

Asst. Prof. Ali Rıfat BOYNUEĞRİ, Member
Yildiz Technical University _____

Asst. Prof. Sıtkı GÜNER, Member
Eskişehir Technical University _____

I hereby declare that I have obtained the required legal permissions during data collection and exploitation procedures, that I have made the in-text citations and cited the references properly, that I haven't falsified and/or fabricated research data and results of the study and that I have abided by the principles of the scientific research and ethics during my Thesis Study under the title of Development of Decision Making Mechanism for Energy Transition Between Electric Vehicles in Parking Lots Considering Vehicle to Vehicle supervised by my supervisor, Assoc. Prof. Ozan ERDİNÇ. In the case of a discovery of false statement, I am to acknowledge any legal consequence.

Hilmi Cihan GÜLDORUM

Signature

This study was supported by the Scientific and Technological Research Council of Turkey (TUBITAK) under project Grant 119E215.

*Dedicated to my family*

# ACKNOWLEDGEMENTS

In this study, the mitigation of increased comfort violation due to demand response programs of electric vehicles parked in electric vehicle parking lot was investigated considering the vehicle-to-vehicle concept.

Firstly, I'd like to express my gratitude to my thesis advisors Assoc. Prof. Ozan ERDİNÇ and Asst. Prof. İbrahim Şengör for their constant inspiration, for their invaluable and continuous support and patience during my study. Their comprehensive knowledge and experience have aided me in both academic research and daily life.

I'd like to express my thanks to my family for their unwavering support throughout my life.

Hilmi Cihan GÜLDORUM

# TABLE OF CONTENTS

**LIST OF SYMBOLS** viii

**LIST OF ABBREVIATIONS** x

**LIST OF FIGURES** xi

**LIST OF TABLES** xiii

**ABSTRACT** xiv

**ÖZET** xvi

**1 INTRODUCTION** 1

1.1 Literature Review . . . . . 2

1.1.1 Review of the Literature on Grid-to-Vehicle (G2V) . . . . . 2

1.1.2 Review of the Literature on Vehicle-to-Grid (V2G) . . . . . 3

1.1.3 Review of the Literature on Vehicle-to-Vehicle (V2V) . . . . . 6

1.2 Objective of the Thesis . . . . . 8

1.3 Original Contribution . . . . . 8

1.4 Thesis Outline . . . . . 9

**2 VEHICLE-TO-EVERYTHING (V2X)** 10

2.1 Vehicle-to-Grid (V2G) . . . . . 11

2.2 Vehicle-to-Vehicle (V2V) . . . . . 15

2.3 Vehicle-to-Home (V2H) and Vehicle-to-Building (V2B) . . . . . 15

**3 METHODOLOGY** 16

3.1 Mathematical Formulation . . . . . 17

3.1.1 Objective Function . . . . . 17

3.1.2 Constraints and Equations of Electric Vehicle . . . . . 17

3.1.3 Constraints and Equations of Electric Vehicle Parking Lot . . . . 19

3.1.4 Determining Electric Vehicle Comfort . . . . . 19

3.2 LSTM Cells . . . . . 20

**4 TEST AND RESULTS** 22

4.1 Input Data . . . . . 22
4.2 Case Studies . . . . . 25
4.3 EVPL Power Variations . . . . . 28
4.4 SoE and Power Variations of EVs . . . . . 33
4.4.1 SoE and Power Variations of the EV - 103 . . . . . 33
4.4.2 SoE and Power Variations of the EV - 166 . . . . . 38
4.4.3 SoE and Power Variations of the EV - 28 . . . . . 41

**5 RESULTS AND DISCUSSION** **44**

**REFERENCES** **46**

**A PYTHON CODES** **54**
A.1 Python Codes for Base Case-1, Base Case-2, Case-1, Case-2, Case-5 and Case 6 . . . . . 54
A.2 Python Codes for Case-3, Case-4, Case-7 and Case-8 . . . . . 57

**PUBLICATIONS FROM THE THESIS** **60**

# LIST OF SYMBOLS

| | |
|---|---|
| $T_n^a$ | Arrival time of electric vehicle $n$. |
| $BatCap_n^{EV}$ | Battery capacity of electric vehicle $n$ [kWh]. |
| $u_n^3$ | Binary variable for comfort violation of electric vehicle $n$. 1 if the comfort of electric vehicle $n$ is violated; else 0. |
| $u_{n,t}^1$ | Binary variable for the charging and discharging state of electric vehicle $n$ in period $t$. 1 if electric vehicle $n$ is charging in period $t$; else 0. |
| $u_t^2$ | Binary variable for the power exchange between grid and parking lot. 1 if parking lot injects power into the grid in period $t$; else 0. |
| $CE_n^{EV}$ | Charging efficiency of electric vehicle $n$ [%]. |
| $P_{n,t}^{EV,ch}$ | Charging power of electric vehicle $n$ in period $t$ [kW]. |
| $Com_Vio_n^{EV}$ | Comfort violation of electric vehicle $n$ [%]. |
| $P_t^{V2G,contract}$ | Contracted Vehicle-to-Grid power in period $t$ [kW]. |
| $T_n^d$ | Departure time of electric vehicle $n$. |
| $SoE_n^{EV,des}$ | Desired State-of-Energy of electric vehicle $n$ [kWh]. |
| $DE_n^{EV}$ | Discharging efficiency of electric vehicle $n$ [%]. |
| $P_{n,t}^{EV,dsch}$ | Discharging power of electric vehicle $n$ in period $t$ [kW]. |
| $SoE_n^{EV,init}$ | Initial State-of-Energy of electric vehicle $n$ [kWh]. |
| $SoE_n^{EV,min}$ | Minimum State-of-Energy of electric vehicle $n$ [kW]. |
| $SoE_n^-$ | Negative value of the difference between final State-of-Energy and desired State-of-Energy of electric vehicle $n$ [kWh]. |
| $P_t^{PV}$ | Photovoltaic production in period $t$ [kW]. |
| $SoE_n^+$ | Positive value of the difference between final State-of-Energy and desired State-of-Energy of electric vehicle $n$ [kWh]. |

| | |
|---|---|
| $P_{n,t}^{EV,V2V_inc}$ | Power drawn from other electric vehicles into electric vehicle $n$ in period $t$ [kW]. |
| $P_{n,t}^{EV,PV2V}$ | Power drawn from photovoltaic into electric vehicle $n$ in period $t$ [kW]. |
| $P_{n,t}^{EV,G2V}$ | Power drawn from the grid into electric vehicle $n$ in period $t$ [kW]. |
| $P_{t}^{G2V}$ | Power drawn from the grid into the parking lot in period $t$ [kW]. |
| $P_{n,t}^{EV,V2V_out}$ | Power injected from electric vehicle $n$ into other electric vehicles in period $t$ [kW]. |
| $P_{n,t}^{EV,V2G}$ | Power injected from electric vehicle $n$ into the grid in period $t$ [kW]. |
| $P_{t}^{PLL,signal}$ | Power limit signal imposed by the system operator in period $t$ [kW]. |
| $n$ | Set of electric vehicles. |
| $t$ | Set of time periods. |
| $SoE_{n}^{EV,final}$ | State-of-Energy of electric vehicle $n$ in departure time [kWh]. |
| $SoE_{n,t}^{EV}$ | State-of-Energy of electric vehicle $n$ in period $t$ [kWh]. |
| $\Delta T$ | Time granularity. |

# LIST OF ABBREVIATIONS

| | |
|---|---|
| DR | Demand Response |
| EV | Electric Vehicle |
| EVPL | Electric Vehicle Parking Lot |
| G2V | Grid-to-Vehicle |
| LSTM | Long Short-Term Memory |
| MAE | Mean Absolute Error |
| MILP | Mixed-Integer Linear Programming |
| PLL | Peak Load Limitation |
| PV | Photovoltaic |
| ReLU | Rectified Linear Unit |
| RMSE | Root Mean Square Error |
| SoE | State-of-Energy |
| V2G | Vehicle-to-Grid |
| V2V | Vehicle-to-Vehicle |

# LIST OF FIGURES

**Figure 2.1** General concept of V2X . . . . . 10
**Figure 3.1** Scheme of proposed EVPL model . . . . . 16
**Figure 3.2** Structure of a LSTM cell . . . . . 21
**Figure 4.1** Comparison of the outputs of the ML model with actual values for temperature, irradiance and EVPL . . . . . 24
**Figure 4.2** Forecasted output power of PV . . . . . 25
**Figure 4.3** Comparison of initial SoE and desired SoE of each EV . . . . . 26
**Figure 4.4** Power drawn from grid in Base Case-1 and Base Case-2 . . . . . 28
**Figure 4.5** Comparison of the power drawn from grid in Case-1 and Case-2 with Base Case-1 and Base Case-2 . . . . . 29
**Figure 4.6** Comparison of the power drawn from grid in Case-3 and Case-4 with Base Case-1 and Base Case-2 . . . . . 30
**Figure 4.7** Comparison of the power drawn from grid in Case-5 and Case-6 with Base Case-1 and Base Case-2 . . . . . 30
**Figure 4.8** Comparison of the power drawn from grid in Case-7 and Case-8 with Base Case-1 and Base Case-2 . . . . . 31
**Figure 4.9** Power drawn from grid and power injected into the grid for all case studies. . . . . 31
**Figure 4.10** V2V power variations . . . . . 32
**Figure 4.11** SoE and power variations of EV-103 (Base Case-1) . . . . . 33
**Figure 4.12** SoE and power variations of EV-103 (Base Case-2) . . . . . 34
**Figure 4.13** SoE and power variations of EV-103 (Case-1 and Case-2) . . . . . 34
**Figure 4.14** SoE and power variations of EV-103 (Case-3) . . . . . 35
**Figure 4.15** SoE and power variations of EV-103 (Case-4) . . . . . 35
**Figure 4.16** SoE and power variations of EV-103 (Case-5) . . . . . 36
**Figure 4.17** SoE and power variations of EV-103 (Case-7) . . . . . 37
**Figure 4.18** SoE and power variations of EV-103 (Case-8) . . . . . 37
**Figure 4.19** SoE and power variations of EV-166 (Base Case-1) . . . . . 39
**Figure 4.20** SoE and power variations of EV-166 (Case-1 and Case-2) . . . . . 39
**Figure 4.21** SoE and power variations of EV-166 (Case-4) . . . . . 40
**Figure 4.22** SoE and power variations of EV-166 (Case-5) . . . . . 40

**Figure 4.23** SoE and power variations of EV-166 (Case-8) . . . . . 41
**Figure 4.24** SoE and power variations of EV-28 (Base Case-1 and Base Case-2) 42
**Figure 4.25** SoE and power variations of EV-28 (Case-8) . . . . . 42

# LIST OF TABLES

**Table 1.1** Literature summary of V2V studies . . . . . 9
**Table 2.1** Practical evidences of V2G across the world . . . . . 12
**Table 3.1** Nomenclature of the proposed model . . . . . 17
**Table 4.1** Data and model properties . . . . . 23
**Table 4.2** Statistics of the EVPL in october . . . . . 26
**Table 4.3** Specifications of EVs that used in case studies . . . . . 27
**Table 4.4** Comparisons of the case studies . . . . . 28
**Table 4.5** Comparison of the results of EVPL for evaluated case studies . . . . 32
**Table 4.6** Comparison of the results of EV-103 in evaluated case studies . . . . 38
**Table 4.7** Comparison of the results of EV-166 in evaluated case studies . . . . 41
**Table 4.8** Comparison of the results of EV-28 in evaluated case studies . . . . . 43

# ABSTRACT

## Development of Decision Making Mechanism for Energy Transition Between Electric Vehicles in Parking Lots Considering Vehicle to Vehicle

Hilmi Cihan GÜLDORUM

Department of Electrical Engineering
Master of Science Thesis

Advisor: Assoc. Prof. Ozan ERDİNÇ
Co-advisor: Asst. Prof. İbrahim ŞENGÖR

The transition from internal combustion engine vehicles to electric vehicles has accelerated significantly in recent years, owing to increased social awareness and incentives for reducing carbon emissions. In comparison to conventional loads, electric vehicles are rather mobile and flexible loads. As a result, in addition to examining the integration of electric vehicles into the distribution system as sole load, academia and industry have focused on the use of electric vehicle batteries in ancillary services to the grid, arbitrage, and reserve operations via services such as vehicle-to-grid, vehicle-to-home, and vehicle-to-building. However, the impact of these services on the comfort of electric vehicles should be minimized in order to encourage electric vehicle owners to participate in these services.

In this thesis, firstly, the effect of vehicle-to-grid power transfer and peak load limitation services on the load profile drawn from the grid and on the comfort violations of the electric vehicle users in the electric vehicle parking lot are examined. Following that, an optimization model in the form of mixed-integer linear programming is developed with the aim of minimizing the unmet energy requirement of electric vehicles through energy transfer between vehicles and photovoltaic generation, so that electric vehicle users are not discouraged from participating in these services due to comfort violation. The uncertainties of photovoltaic production and electric vehicles are taken into account with high accuracy using real data by designing a machine learning model based on long short-term memory cells, which

is a special type of recurrent neural networks. The proposed optimization model was developed with the Python programming language, solved with the Gurobi commercial solver , and tested with 10 case studies. Examining the results, it can be seen that comfort violations caused by vehicle-to-grid and peak load limitation services can be successfully mitigated through vehicle-to-vehicle and photovoltaic generation.

**Keywords:** Demand response, electric vehicles, recurrent neural networks, vehicle-to-grid, vehicle-to-vehicle

# ÖZET

## Elektrikli Araç Park Bölgelerinde Araçlar Arasında Enerji Aktarımı İçin Karar Verme Mekanizmasının Geliştirilmesi

Hilmi Cihan GÜLDORUM

Elektrik Mühendisliği Anabilim Dalı
Yüksek Lisans Tezi

Danışman: Doç. Dr. Ozan ERDİNÇ
Eş-Danışman: Dr. Öğr. Üyesi İbrahim ŞENGÖR

Son yıllarda, karbon emisyonunun azaltılması konusunda toplumsal farkındalığın ve verilen teşviklerin arması ile içten yanmalı motorlu araçlardan elektrikli araçlara geçiş önemli ölçüde hızlanmıştır. Elektrikli araçlar, günümüzde klasik anlamdaki yüklerden farklı olarak oldukça mobil ve esnek yüklerdir. Bu nedenle, elektrikli araçların sadece yük olarak dağıtım sistemine entegrasyonunun incelenmesi yanında aynı zamanda elektrikli araç bataryalarının araçtan şebekeye güç aktarımı, araçtan eve güç aktarımı, araçtan binaya güç aktarımı gibi servislerle şebekeye yardımcı servislerde, arbitraj ve rezerv işlemlerinde kullanılması akademi ve endüstrinin yoğun ilgisini çekmektedir. Ancak, elektrikli araç sahiplerinin bu servislere katılımının sağlanması için, bu servislerin elektrikli araçların konforuna olan etkisi en aza indirilmelidir.

Bu tezde, ilk olarak araçtan şebekeye güç aktarımı ve pik yük kısıtlaması servislerinin şebekeden çekilen yük profiline ve elektrikli araç parklanma bölgesinde bulunan elektrikli araç kullanıcılarının konfor ihlallerine etkisi incelenmiştir. Sonrasında, elektrikli araç kullanıcılarının bu servislere katılımı konusunda konfor bozulması nedeniyle tereddüt etmemesi için araçlar arası enerji aktarımı ve fotovoltaik üretim kullanılarak elektrikli araçların karşılanamayan enerji ihtiyacını en aza indirgemeyi amaçlayan karmaşık tam sayılı doğrusal programlama formunda bir optimizasyon modeli oluşturulmuştur. Fotovoltaik üretim ve elektrikli araçların belirsizlikleri, tekrarlayan yapay sinir ağlarının özel bir türü olan uzun kısa süreli hafıza hücreleri temelli bir makine öğrenmesi modeli tasarlanarak gerçek verilerle birlikte yüksek

doğrulukta dikkate alınmıştır. Önerilen optimizasyon modeli Python programlama dili ile geliştirilmiş, Gurobi ticari çözücüsü ile çözülmüş ve 10 vaka çalışması ile test edilmiştir. Sonuçlar incelendiğinde, araçtan şebekeye güç aktarımı ve pik yük kısıtlanması servislerinin neden olduğu konfor bozulmasının araçlar arası güç aktarımı ve fotovoltaik üretim yardımıyla başarıyla azaltıldığı görülmüştür.

**Anahtar Kelimeler:** Talep yanıtı, elektrikli araçlar, tekrarlayan sinir ağları, araçtan-şebekeye güç aktarımı, araçtan-araca güç aktarımı

# 1
# INTRODUCTION

In recent years, climate change as a result of the accumulation of greenhouse gases (GHG) has emerged as one of humanity's most serious problems. Although carbon dioxide ($CO_2$) emissions have decreased as a result of decreased energy demand during the 2020 pandemic period, global $CO_2$ emissions related to energy have been increasing since the 1900s and are likely to continue to do so unless drastic changes are implemented [1]. The transportation sector is responsible for 23% of global $CO_2$ emissions related to energy [2] . Electric vehicles (EVs) will inherently play a significant role in reducing $CO_2$ emissions.

The role of EVs in our lives has expanded rapidly as countries pursue policies aimed at transitioning to zero-carbon transportation systems in order to reduce $CO_2$ emissions, as well as tax and purchase incentives for EVs, a diverse range of EV models, and price reductions due to advances in battery technology. According to the International Energy Agency's EV Outlook 2021 report, 14 billion dollars were invested in EVs as an incentive in 2020, and 10 million EVs are currently in circulation on the roads. By 2030, the number of EVs is expected to range between 145 million and 230 million, depending on the various scenarios [3]. Furthermore, EV energy demand is expected to reach 550 TWh by 2030, which is six times higher than in 2019 [3]. In Turkey, it is anticipated that EV sales will total between 300,000 and 800,000 units by 2030 [4]. However, an increase in EV energy demand may result in negative power quality effects such as supply-demand imbalance, voltage fluctuation, harmonic problems, and system asset overloading in the power system [5]. As a result, EV integration into the power system has become a crucial research topic in order to mitigate the negative effects and investigate the potential benefits of EVs as ancillary services to the power system [6].

## 1.1 Literature Review

Numerous studies have been conducted in recent years to examine the integration of EVs into power systems. This section examines studies that are relevant to this thesis.

### 1.1.1 Review of the Literature on Grid-to-Vehicle (G2V)

Kuran et al. [7] proposed a two-stage multi-objective optimization model aiming at maximizing the electric vehicle parking lot (EVPL) owner's revenue and minimizing the EV owner's unmet energy requirement while accounting for the various EV patterns. Additionally, this study considered peak load limitation (PLL) operation in relation to the grid's requirements. Akhavan-Rezai et al. [8] proposed a nonlinear mixed-integer programming model for charge planning with the aim of maximizing the comfort of EVs in terms of energy supplied by prioritizing EVs coming to an EVPL using fuzzy logic based on their technical characteristics and departure times. Şengör et al. [9] proposed a stochastic mixed-integer linear programming (MILP) model that aims to maximize the load factor of an EVPL through PLL-based demand response (DR) program that takes into account the arrival times and initial State-of-Energy (SoE) uncertainties of the EVs using different driving patterns. However, in this model, it was assumed that EVs would achieve the desired charge level at departure time. And also in [10], Sengör et al. developed a load factor maximization oriented real-time optimization strategy in EPVL. In [10] , historical data was used to account for the uncertainties associated with EVs, and PLL operation and fast charging were also examined. Zhang et al. [11] investigated the optimal planning of an EVPL using a two-stage stochastic optimization model in which annual investment and operation costs are minimized in the first stage and the effects of coordinated charging are investigated in the second stage. Jiang et al. [12] examined a real-time optimization model in the form of a MILP to minimize operational costs by charging scheduling in an EVPL equipped with photovoltaic (PV) and additional battery storage. PV and EV uncertainties were considered and solved using the gray wolf optimization method, which is a meta-heuristic approach. Zhang et al. [13] proposed a two-stage optimization model that examines the optimum EVPL operation both in the short term and in the long term, where the costs of an EVPL are minimized in the short term with linear programming and in the long term with Approximate Dynamic Programming. Furthermore, the unmet energy requirements of EVs were taken into account with the penalty fee. Chen et al. [14] proposed a two-stage stochastic programming model that aims to minimize investors' EVPL investment and maintenance costs by accounting for the various types of EVPLs. Additionally, the unmet energy requirement of EV was considered with a penalty cost. Zhang et al. [15] proposed model predictive control-based real-time optimization study to maximize profit in an EVPL equipped

with PV. While the uncertainties associated with EV and PV were considered in this study, the preferences of EV owners were not considered, and it was assumed that the EVs reached the desired charge level at the departure time. Awad et al. [16] investigated co-operation of EV, distributed generation, and battery storage in EVPLs by developing a decision-making mechanism for renewable energy source (RES) and battery storage sizing, EV charging, charging price bidding decisions in coordinated and uncoordinated charging situations using a model aimed at maximizing an EVPL owner's annual income. Jannati et al. [17] presented a multi-objective optimization model for scheduling charging in an EVLP equipped with RES and hydrogen storage in order to minimize total cost and carbon emissions. The proposed study was solved using the weighted sum method.

Fallah-Mehrjardi et al. [18] developed a multi-stage optimization model for charging scheduling in an EVPL. The distribution transformer limits, battery capacities, and uncertainties in the arrival, departure, and demand of the vehicles were all taken into account in detail, and unmet energy requirements were penalized in the proposed model, which was solved using Stochastic Dual Dynamic Programming. Rahmani-Andebili et al. [19] investigated the optimal planning and operation of an EVPL from the perspective of both the distribution and generation companies. While the distribution company sought to minimize line losses and total cost in this study, the generation company sought to maximize profits through optimal EVPL operation. Additionally, the preferences and driving patterns of EV owners were considered. Zeng et al. [20] researched the long-term optimal placement of EVPL taking into account the distribution system constraints while examining the impact of all EV owner uncertainties on incentive-based DR programs. The proposed model was developed in the form of a two-stage stochastic optimization problem and solved using genetic algorithm. Xie et al. [21] proposed a bilevel optimization model in which a company with an EV fleet and an EVPL at the upper level aims to maximize its revenue through optimal pricing and charging planning, while market-clearing occurs at the lower level. Additionally, taking into account line losses, optimal power flow was conducted and solved using convex relaxation to optimize market clearing.

### 1.1.2 Review of the Literature on Vehicle-to-Grid (V2G)

Li et al. [22] proposed an optimization study aimed at minimizing load fluctuations in the distribution network via V2G by controlling the charging and discharging transactions of EVs while preserving the users' private information via a hyperledger structured consortium blockchain-based approach. The proposed model was constructed using the MILP formulation and solved using the Krill Herd algorithm.

By reaching 90 percent of their battery capacity in departure time, EVs maintained their comfort. Moradijoz et al. [23] proposed a bilevel optimization model for distribution extension planning in which the upper level maximizes revenue for the distribution system operator (DSO) considering distribution loss and investment costs, and the lower level maximizes revenue for the EVPL while taking into account charging and discharging planning. Mirzaei et al. [24] proposed the optimal placement and capacity planning of an EVPL in the distribution system, utilizing an optimization model that maximizes revenue from charging and discharging operations while minimizing land and maintenance costs considering the EV owners' various driving patterns. However, this study did not examine EVs that failed to be charged to the desired level. To examine the optimal location of an EVPL in the distribution system, Neyestani et al. [25] developed a two-stage multi-objective optimization model in which the investment cost, loss cost, and voltage deviation cost were minimized in terms of DSO in the first stage and the EVPL revenue was maximized in the second stage. Also, in this study, the uncertainties associated with EV, RES, and electricity prices were taken into account. Shafie-Khah et al. [26] implemented a stochastic multi-stage two-level optimization model, in which EVPL tries to maximize its revenues by participating in reserve and ancillary services in the first layer and aims to minimize the cost of DSO's regulation services and renewable energy spillage in the second layer. In [26] , It was assumed that each EV reached the desired charge level. In a solar-equipped EVPL, Deb et al. [27] proposed a charging scheduling model in which the overall cost is tried to be minimized with V2G and G2V. The gradient boosting approach was used to try to resolve the SoE uncertainties associated with EVs in the proposed model. With 800 EV in a 38-bus radial system, the highest EV penetration without causing congestion was investigated, and the proposed model was developed using particle swarm optimization. As a result, global optimality was not ensured. Zeng et al. [28] proposed a two-stage stochastic optimization model in which the optimal placement, sizing, and contracts for the EVPL are determined in the first stage and operation costs are examined in the second stage, with the aim of maximizing an EVPL's annual profit while taking distribution system constraints, direct current optimal power flow constraints, Quality of Service constraints, and V2G into account. In this study, it was assumed that EVs reached the desired charge level at the time of departure. Yazdani-Damavandi et al. [29] suggested a stochastic model in which a system operator in charge of multiple energy sources maximizes its own revenue through electricity, gas, V2G, and reserve operations while taking the EVPL concept and EV uncertainties into account. Neyestani et al. [30] developed a bilevel optimization model in which an aggregator in charge of managing distributed generation, EVPL, and commercial loads aims to maximize profits by interacting with the network while taking distribution system constraints and power flow into account,

and the EVPL owner aims to maximize revenue at the lower level. Singh et al. [31] developed a model aimed at minimizing distribution system losses by scheduling the charging and discharging of V2G-equipped EVs. Additionally, cost-benefit analysis and reconfiguration of the distribution system using various strategies, and uncertainties of EVs were examined. Huang et al. [32] studied two different models using internal point optimization to maximize total peak load shift and minimize total cost considering power loss, charging and discharging fees, degradation cost, voltage control, and three-phase optimal power flow. At the departure time, it was assumed that all EVs reach their desired SoE. Tavakoli et al. [33] analyzed a bilevel optimization model in the form of MILP in which an EV aggregator and a company that owns wind farms and conventional energy production aim to maximize their revenues by participating in regulation services at the upper level and to maximize social welfare for market clearing at the lower level. Huang et al. [34] investigated the elimination of congestion from a distribution system using positive and negative charges in a distribution system with a high proportion of PV, heat pumps, and EVs equipped with V2G. The proposed model was deterministically validated using the predicted data and distributedly solved using dual decomposition. Sadati et al. [35] proposed a bilevel optimization model based on Conditional Value at Risk (CVaR) where at the upper level, the distribution company aims to maximize its profits with EVPL and upstream grid interactions, at the lower level, the EVPL owner aims to maximize its revenue with EV and distribution company interactions. Salyani et al. [36] developed a non-cooperative Stackelberg Game model in which the distribution company aims to maximize its earnings as the leader, while the EVs in EVPL attempt to maximize their earnings as followers by participating in DR programs such as load shifting and V2G.

Vosoogh et al. [37] developed an energy management model aimed at minimizing overall costs in microgrids that incorporate RES, EVs, and battery storage in order to mitigate the negative effects of EVs. The proposed model was solved using the modified bat algorithm, and the RES uncertainties were considered using support vector machines and the point estimate method. Ebrahimi et al. [38] developed a two-stage stochastic charging and discharging planning model for residential areas with the goal of minimizing charging costs while maintaining EV comfort by taking into account battery degradation cost, waiting time, and meeting their demands. Neyestani et al. [39] developed a model focused on EV and market interaction with the goal of maximizing the profits of the aggregator that manages charging stations and EVPL. The power flow was examined in detail in the proposed model by considering traffic flow models of EVs that travel between different residential areas. However, flexibility in terms of SoE at the time of departure was not suggested in

this study. Kumar Nunna et al. [40] conducted an energy management study in the form of a multi-agent system in microgrids with significant energy imbalances and price volatility, taking V2G operation into account. The purpose of this study was to minimize supply-demand imbalances in the case of inaccurate load forecasting and to maximize revenue from V2G. Additionally, battery degradation was taken into account. Chen et al. [41] proposed a game theory-based model in which EVs aim to maximize their profits by participating in regulation services (V2G), the EV aggregator aims to maximize its profits, and all EVs aims to maximize social welfare in the cooperative case. Maigha et al. [42] conducted a multi-objective optimization study in residential parking lots with the goal of minimizing charging and battery aging costs associated with V2G and maximizing the parking lot's load factor by reducing power deviations. The augmented -constraint method was used to solve the proposed model. Chandra Mouli et al. [43] investigated the cost minimization management strategy for EV charging and discharging operations in a parking lot equipped with PV, as well as the participation of EVs in up- and down-regulation regulation services via V2G. MILP was used to formulate the proposed study, and PV uncertainties were considered by model predictive control.

### 1.1.3 Review of the Literature on Vehicle-to-Vehicle (V2V)

Sánchez-Martín et al. [44] examined the effects of valley filling, V2G and V2V in household, commercial and mixed areas in terms of minimizing global cost and maximizing the energy supplied to EV batteries according to the electricity price signal. Unmet energy requirements were penalized and depth of discharge of battery was taken into account. Nevertheless, V2G , and V2V were not regarded as applicable due to battery constraints.

Wang et al. [45] developed an energy swap station model that aims to minimize the charging cost and maximize the discharging revenue. The proposed model was designed as a semi-distributed optimization problem in which swap stations optimize energy exchange prices centrally and EVs optimize discharging and charging decisions in a distributed manner. However, the swapping stations were considered to serve only as energy exchange stations and were not connected to the grid. In [46], [45] was improved considering grid-to-vehicle and multiple swapping station aggregators and their effects on the distribution system. However, the proposed model was designed in the form of mixed-integer nonlinear programming and as a result of this, global optimality was not guaranteed.

You et al. [47, 48] suggested an optimal charging and discharging scheduling structure for an EVPL with V2V capability. The goal of these researches, which were formulated

as MILP and solved in a distributed manner using dual and benders decomposition, was to minimize the social cost. Also, PLL and battery degradation were considered.

Alvaro et al. [49] studied a parking area that tries to minimize the charging cost with V2V by bringing together EVs with excess energy and EVs that wanted to be charged in the same parking area. However, V2G, PLL , and PV were not considered.

Koufakis et al. [50] presented a study aiming to increase the user comfort in terms of reaching the desired State-of-Energy (SoE) value and reduce the number of energy transactions by using V2G, V2V, PV, and additional backup batteries. However, the study in [50] did not include PV and EV parking forecasts and PLL. Also in [51], extended version of [50], Koufakis et al. presented both online and offline optimization concepts with the aim of minimizing the charging cost and increasing RES usage by V2V transactions and virtual demand. RES forecast was performed using the k-nearest neighbors algorithm. Nevertheless, V2G and PLL were not considered in this study. Both studies were formulated as MILP problem.

Kang et al. [52] proposed a social welfare maximization-oriented platform for local energy trading among EVs in parking stations based on a consortium blockchain. However, V2G, PV, and PLL were not taken into account in this study.

Network welfare maximization oriented EV matching algorithm for energy transactions between EVs was proposed by Zhang et al. In this study [53], EVs were divided into two as providing energy and receiving energy by weighted bipartite graph and the matching problem was solved through the max-weight algorithm. Nevertheless, V2G, PLL, and PV were not considered.

Li et al. [54] investigated the optimal route and charging location selection for EVs participating in the V2V process, taking into account the EVs' communication protocols. The proposed model was developed using reinforcement learning and a weighted bipartite graph algorithm. The EVs' arrival time uncertainty was resolved using an Long Short-Term Memory (LSTM)-based forecast algorithm.

Huang et al. [55] presented a consortium blockchain-based multi-objective optimization model in which EVs' satisfaction is maximized and charging cost is minimized considering EVs route selection. In this study, user satisfaction was defined in terms of the mismatch between desired energy and actual energy. The proposed model was solved with the Non-Dominated Sorting Genetic Algorithm (NDSA). However, V2G, PLL, and PV were not mentioned. Zeng et al. [56] developed a bipartite graph matching-based model for energy exchange between EVs with aim of minimizing charging cost and maximize discharging cost. The proposed model

was solved with particle swarm optimization method that did not guarantee global optimality. Although in [56], V2G and wind generation were taken into account, PLL and comfort maximization were not considered.

Chacko et al. [57] developed a charging station equipped with PV and backup batteries to reduce the negative impacts of EVs on the electrical grid. The proposed study was designed as a multi-objective optimization model with the aim of minimizing EV charging costs and maximizing EV revenues while also minimizing emission levels of plug-in hybrid electric vehicles (PHEV).

Al-Obaidi et al. [58] proposed a peer-to-peer energy trading and V2G method for EVs that utilizes model predictive control to maximize total revenue and minimize total charging costs. However, the EVPL concept and PV were not considered.

Mozaffari et al. [59] proposed a multi-objective optimization model that examines optimum long-term distribution system expansion planning and optimum EVPL siting. The proposed model aimed to maximize the EVPL owner's income by considering the charging and discharging fees, investment, operation, and maintenance costs, and minimizing the costs of the distribution system in terms of maintenance, operation, and loss costs. In this study, it was assumed that all EVs reach their desired SoE value at the departure time. Also, uncertainties of EVs were considered by a forecasting algorithm.

Although the reviewed studies provide valuable contributions to the existing literature, the effect of V2V in the EVPL concept has not been adequately investigated.

## 1.2 Objective of the Thesis

In this thesis, the effect of V2V and PV to mitigate the comfort violation of EVs during V2G and PLL operations in EVPL was investigated and modeled within MILP framework in the day-ahead market. The main purpose of the proposed model is to reduce the comfort violation of EVs in the EVPL. This thesis discusses the comfort of EVs in terms of reaching the desired SoE level.

## 1.3 Original Contribution

The contributions of this thesis can be summarized as follows:

- This thesis is the first study that aims to maximize user comfort by taking V2G, V2V, PLL, and PV into consideration.

- Uncertainties in the arrival time and the parking time of EVs together with PV production were considered using LSTM cells that a special kind of Recurrent Neural Network (RNN).

Table 1.1 highlights the distinctions between this thesis study and other V2V studies published in the literature.

**Table 1.1** Literature summary of V2V studies

| References | Author | Year | EVPL | V2G | V2V | PLL | RES | Forecast | |
|---|---|---|---|---|---|---|---|---|---|
| | | | | | | | | RES | EV |
| [44] | Sanchez-Martin et al. | 2012 | ✓ | ✓ | ✓ | - | - | - | - |
| [45] | Wang et al. | 2014 | - | - | ✓ | - | - | - | - |
| [47] | Pengcheng-You et al. | 2014 | - | - | ✓ | ✓ | - | - | - |
| [49] | Alvaro et al. | 2014 | - | - | ✓ | - | - | - | - |
| [48] | Pengcheng-You et al. | 2016 | - | - | ✓ | ✓ | - | - | - |
| [50] | Kouafakis et al. | 2016 | - | ✓ | ✓ | - | - | - | - |
| [52] | Kang et al. | 2017 | ✓ | - | ✓ | - | - | - | - |
| [46] | Wang et al. | 2018 | ✓ | - | ✓ | - | - | - | - |
| [53] | Zhang et al. | 2019 | ✓ | - | ✓ | - | - | - | - |
| [54] | Li et al. | 2019 | - | - | ✓ | - | - | - | ✓ |
| [55] | Huang et al. | 2019 | - | - | ✓ | - | - | - | - |
| [51] | Kouafakis et al. | 2020 | - | - | ✓ | - | ✓ | ✓ | - |
| [56] | Zeng et al. | 2021 | - | ✓ | ✓ | - | ✓ | - | - |
| [57] | Chacko et al. | 2021 | - | - | ✓ | - | ✓ | - | - |
| [58] | Alobaidi et al. | 2021 | - | ✓ | ✓ | - | - | - | - |
| This Thesis | H. Cihan Güldorum | 2021 | ✓ | ✓ | ✓ | ✓ | ✓ | ✓ | ✓ |

## 1.4 Thesis Outline

The remainder of the thesis is organized as follows. Chapter 2 encapsulates an overview of the Vehicle-to-Everything. Chapter 3 presents the mathematical formulation of the proposed optimization model. Afterward, the processing of the input data, conducted test studies, and results are analyzed in Chapter 4. The outcomes of this thesis study are summarized in Chapter 5 along with potential future research directions.

# 2
# VEHICLE-TO-EVERYTHING (V2X)

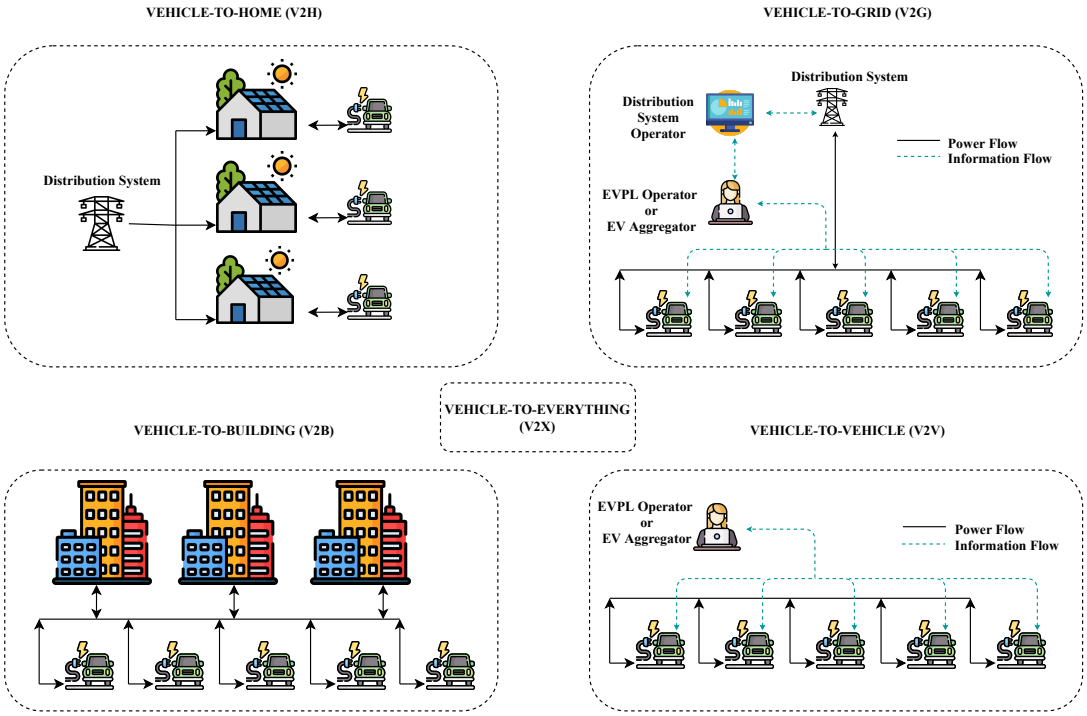



**Figure 2.1** General concept of V2X

In recent years, researchers have focused their attention on the use of EV batteries in ancillary activities to power systems using the Vehicle-to-Everything (V2X) concept. Figure 2.1 illustrates the general concept of V2X. With V2G, which is a subset of the V2X concept, EV batteries contribute to the distribution system's reliability through arbitrage operations, acting as an energy source in regulation services, reactive power support operations, and PLL operations. Thanks to the V2H function, EV batteries can be used as a backup storage system, arbitrage and load shifting entity with the aim of cost minimization, and load deviation minimization. In the V2V transaction, EVs can

reduce regional price tariffs by transferring energy to each other [60] . In this thesis, V2G and V2V processes in an EVPL have been considered.

## 2.1 Vehicle-to-Grid (V2G)

V2G refers to EVs supporting the electricity grid's balance through bidirectional chargers in response to signals from system operators or aggregators while parked. The services that EVs can provide to various parties can be classified as Transmission System Operator (TSO) services, DSO services, and RES services [61]. These services are as follows:

- TSO Services
  - *Frequency Response and Reserve :* It refers to the actions taken to protect the system's frequency within seconds in the event of supply (Generation) and demand (Load) imbalances in the electrical grid. A reserve is the energy required for frequency operations with a response time longer than one minute [62]. Where production exceeds consumption, EVs participate in the down-regulation service. Otherwise, EVs participate in the up-regulation service [63].
  - *Congestion Management:* It refers to usage of EVs to easing congestion caused by supply and demand exceeding transmission line capacity.
  - *Black Start Provision:* It refers to the use of EV batteries to restore the electrical system following a blackout or other emergency situation.
- DSO Services
  - *Congestion management:* Congestion occurs when supply and demand exceed the technical capacity of the power system components on the line as a result of problems such as overloading or faults. Thanks to the coordinated charging, EVs can help maintain the stability of the electricity grid during times of congestion.
  - *Loss minimization:* Considering the distribution system constraints, line losses can be minimized through loss minimization oriented smart EV charging algorithms.
  - *Load shifting:* It refers to the shifting of loads from peak hours to off-peak hours. Peak-hour charging can be shifted to off-peak hours if it is feasible in terms of the EVs' departure time.

- *Peak shaving and valley filling:* It expresses peak power management operations such as PLL or peak load reduction.
- *Voltage control:* It is to assist the electricity grid's operation by conducted a coordinated charging/discharging model that takes grid voltage constraints into account.

- RES Services
  - *Smooth grid integration and energy curtailment reduction:* It refers to the use of EV batteries to compensate for power system problems caused by the intermittent and variable nature of renewable energy sources.

On the other hand, as illustrated in Table 2.1, there are practical V2G applications involving over 5900 chargers in 86 projects across 22 countries [62] .

**Table 2.1** Practical evidences of V2G across the world [62]

| Location | Number of the chargers | Services |
|---|---|---|
| Australia, Australia | 51 | Frequency Response, Reserve |
| Belgium, Europe | 22 | Frequency Response, Reserve, Load shifting |
| Belgium, Europe | 40 | Frequency Response |
| Canada, North America | 21 | Distribution Services, Load shifting |
| Canada, North America | 1 | Distribution Services, Load shifting, Emergency back-up |
| China, Asia | 5 | Frequency Response, Load shifting, Emergency back-up |
| Germany, Europe | 1 | Load shifting |
| Germany, Europe | 20 | Frequency Response |
| Denmark, Europe | 50 | Frequency Response, Distribution Services, Arbitrage |
| Denmark, Europe | 10 | Frequency Response |

**Table 2.1** Practical evidences of V2G across the world [62] (continued)

| | | |
|---|---|---|
| Spain, Europe | 6 | Load shifting,<br>Power balancing and<br>Power quality support |
| France, Europe | 15 | Frequency Response,<br>Arbitrage,<br>Load shifting |
| France, Europe | 1 | Frequency Response,<br>Distribution Services,<br>Load shifting,<br>Emergency back-up,<br>Arbitrage |
| United Kingdom, Europe | 1 | Frequency Response,<br>Load shifting |
| United Kingdom, Europe | 135 | Arbitrage,<br>Distribution Services,<br>Load shifting,<br>Emergency back-up |
| United Kingdom, Europe | 2 | Arbitrage,<br>Distribution Services,<br>Load shifting |
| United Kingdom, Europe | Unknown | Frequency Response,<br>Arbitrage,<br>Distribution Services,<br>Load shifting |
| United Kingdom, Europe | Unknown | Frequency Response,<br>Arbitrage,<br>Load shifting |
| United Kingdom, Europe | Unknown | Frequency Response,<br>Distribution Services,<br>Load shifting |
| United Kingdom, Europe | Unknown | Frequency Response,<br>Arbitrage,<br>Load shifting |
| United Kingdom, Europe | 35 | Arbitrage,<br>Load shifting |

**Table 2.1** Practical evidences of V2G across the world [62] (continued)

| | | |
|---|---|---|
| United Kingdom, Europe | 6 | Frequency Response, Arbitrage, Load shifting |
| United Kingdom, Europe | 100 | Reserve, Load shifting, Distribution Services |
| United Kingdom, Europe | 2 | Load shifting, Emergency back up |
| United Kingdom, Europe | 330 | Arbitrage |
| United Kingdom, Europe | 2 | Load shifting, Emergency back up |
| United Kingdom, Europe | 4 | Load shifting |
| United Kingdom, Europe | 4 | Reserve, Distribution services, Load shifting |
| Italy, Europe | 600 | Frequency Response |
| Japan, Asia | 4000 | Load shifting, Emergency back up |
| Japan, Asia | 5 | Load shifting, Emergency back up |
| Namibia, Africa | 2 | Load shifting |
| Netherlands, Europe | 2 | Load shifting |
| Netherlands, Europe | 10 | Frequency Response |
| Netherlands, Europe | 1 | Load shifting |
| Netherlands, Europe | 4 | Distribution services, Arbitrage |
| Netherlands, Europe | 80 | Arbitrage |
| Netherlands, Europe | 80 | Frequency Response, Distribution services, Load shifting |
| Netherlands, Europe | 14 | Frequency Response, Distribution services, Load shifting, Emergency back up |
| Netherlands, Europe | 22 | Distribution services, Load shifting |

## 2.2 Vehicle-to-Vehicle (V2V)

V2V is the exchange of energy stored in the batteries of EVs. The functional benefits of V2V can be summarized as follows [60] :

- Serving as a source of energy for other EVS
- Reducing the cost of charging for EV owners during peak times
- Helping coordinated charging algorithms of EVs

## 2.3 Vehicle-to-Home (V2H) and Vehicle-to-Building (V2B)

The V2H and V2B concepts are based on the idea that EVs can assist in the energy management of a home or building by using bidirectional chargers when necessary. While the V2H concept generally features a single EV, the V2B concept includes the presence of multiple EVs in a parking lot. The features of V2H and V2B can be summarized as follows [60]:

- EV batteries can serve as a backup generator.
- EVs can participate in DR programs such as load shifting, valley filling, load peak limitation, and peak load reduction by serving as deferrable/interruptible load.
- It enables EV owners to profit from the arbitrage process, which involves charging the EV battery while the electricity tariff is cheap and discharging it when the tariff is expensive.

# 3
# METHODOLOGY

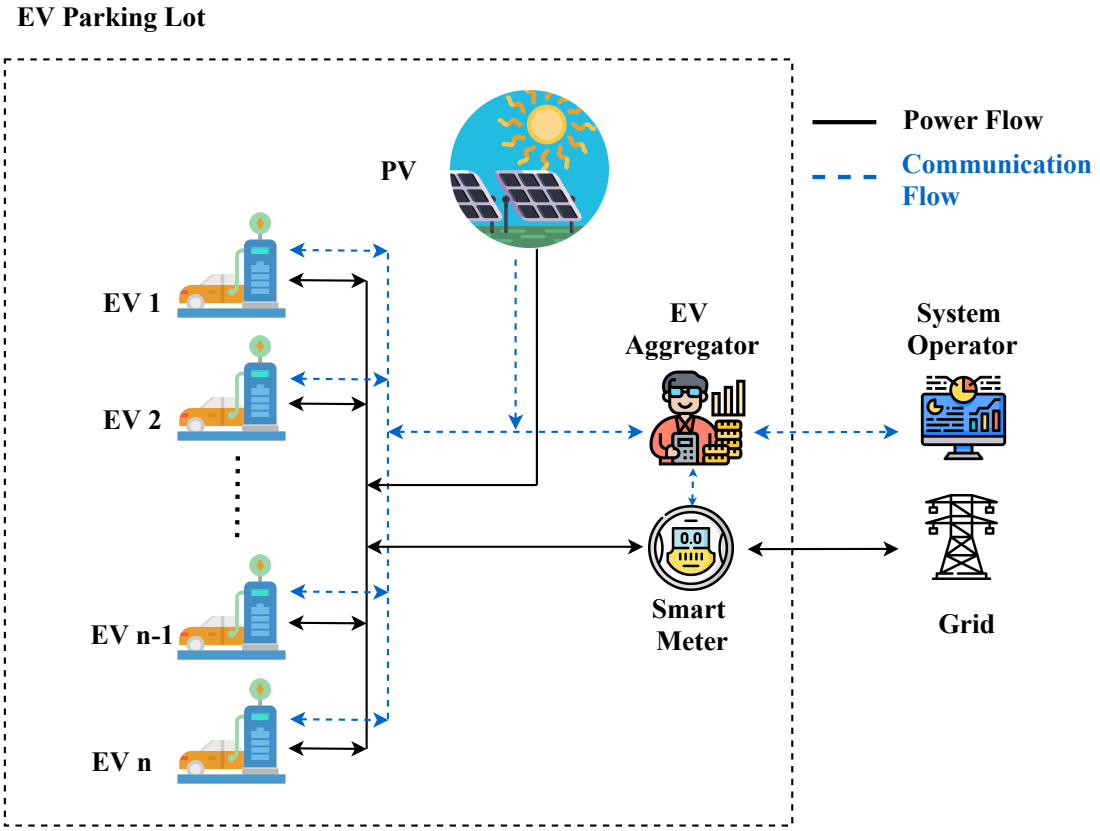



**Figure 3.1** Scheme of proposed EVPL model

The devised model is shown in Figure 3.1. The proposed EVPL is publicly accessible and EV owners may park their vehicles at any time of the day. It should be stated that the EV aggregator makes a V2G agreement with the system operator in the day-ahead market by forecasting the arrival time and parking time of the EVs and the energy to be produced from the PV. The system operator may limit the peak power of EVPL if required through PLL operation. Each EV is assumed to have the capability of both V2V and V2G and could participate in all transactions. It is needed to be highlighted that PV generation is primarily used to charge EVs, thus it is not injected directly into the grid. Furthermore, battery degradation is beyond the scope of this study.

**Table 3.1** Nomenclature of the proposed model

| | |
|---|---|
| **Sets** | $n$, $t$ |
| **Parameters** | $BatCap_n^{EV}$, $CE_n^{EV}$, $DE_n^{EV}$, $P_t^{PLL,signal}$,$P_t^{V2G,contract}$, $P_t^{PV}$,$SoE_n^{EV,des}$, $SoE_n^{EV,init}$, $SoE_n^{EV,min}$, $T_n^a$, $T_n^d$, $\Delta T$ |
| **Variables** | $Com_Vio_n^{EV}$, $P_{n,t}^{EV,ch}$, $P_{n,t}^{EV,dsch}$, $P_{n,t}^{EV,G2V}$, $P_t^{G2V}$, $P_{n,t}^{EV,V2G}$,$P_{n,t}^{EV,PV2V}$, $P_{n,t}^{EV,V2V_inc}$, $P_{n,t}^{EV,V2V_out}$, $SoE_n^+$, $SoE_n^-$, $SoE_{n,t}^{EV}$, $SoE_n^{EV,final}$, $u_{n,t}^1$, $u_t^2$, $u_n^3$ |

## 3.1 Mathematical Formulation

In this study, the developed model is designed as an optimization problem in the form of MILP. The optimization problem aims to provide more system flexibility by minimizing the comfort violation in EV owners' charging experience to enhance the willingness of EV owners to participate in DR programs. The nomenclature of the proposed model is depicted in Table 3.1.

### 3.1.1 Objective Function

The objective function of the developed model is defined in (3.1). The propounded model aims to reduce the average comfort violation. The definition of comfort violation of an EV is expressed by (3.2). The comfort violation is defined as the percentage of the unmet energy requirement of the related EV to the battery capacity. In (3.2), relative comfort violation is calculated for each EV.

$$\textbf{Minimize } \textit{Average Comfort Violation} = \frac{\sum Com_Vio_n^{EV}}{Total\ Number\ of\ EVs} \tag{3.1}$$

$$Com_Vio_n^{EV} = \frac{SoE_n^-}{BatCap_n^{EV}} * 100, \quad \forall n \tag{3.2}$$

### 3.1.2 Constraints and Equations of Electric Vehicle

Inequalities (3.3-3.4) describe that the charging power ($P_{n,t}^{EV,ch}$) and the discharging power ($P_{n,t}^{EV,dsch}$) of each EV cannot be greater than the maximum charging rate ($CR_n^{EV}$) and the maximum discharging rate ($DR_n^{EV}$) of the related EV $n$ during parking period.

$$P_{n,t}^{EV,ch} \leq CR_n^{EV}, \quad \forall n, t \in (T_n^a, T_n^d] \tag{3.3}$$

$$P_{n,t}^{EV,dsch} \leq DR_n^{EV}, \quad \forall n, t \in (T_n^a, T_n^d] \tag{3.4}$$

Equation (3.5) describes that the change of SoE depending on the charging energy amount ($CE_n^{EV} * P_{n,t}^{EV,ch} * \Delta T$) drawn from the grid, PV and other EVs or the discharging energy amount ($P_{n,t}^{EV,dsch} * \Delta T / DE_n^{EV}$) injected to the grid and other EVs in each time interval.

$$\begin{aligned} SoE_{n,t}^{EV} = SoE_{n,t-1}^{EV} + CE_n^{EV} * P_{n,t}^{EV,ch} * \Delta T - \\ P_{n,t}^{EV,dsch} * \Delta T / DE_n^{EV}, \quad \forall n, t \in (T_n^a, T_n^d] \end{aligned} \tag{3.5}$$

Inequality (3.6) keeps the SoE ($SoE_{n,t}^{EV}$) of each EV between minimum ($SoE_n^{EV,min}$) and maximum ($SoE_n^{EV,max}$) boundaries to ensure that the EV battery performs in the safe operating range. Equation (3.7) states that the remaining SoE ($SoE_{n,t}^{EV}$) of EV at arrival time is assumed as initial SoE ($SoE_n^{EV,init}$).

$$SoE_n^{EV,min} \leq SoE_{n,t}^{EV} \leq SoE_n^{EV,max}, \forall n, t \in [T_n^a, T_n^d] \tag{3.6}$$

$$SoE_{n,t}^{EV} = SoE_n^{EV,init}, \quad \forall n, \; if \; t = T_n^a \tag{3.7}$$

Equation (3.8) expresses that the charging power of each EV at time $t$ ($P_{n,t}^{EV,ch}$) equals to the sum of the power drawn from the grid ($P_{n,t}^{G2V}$), other EVs ($P_{n,t}^{V2V,inc}$), and PV ($P_{n,t}^{PV}$). It is noteworthy that PV production is just used to charge EVs, so the selling back to the grid option has not been evaluated in the scope of this work.

$$P_{n,t}^{EV,ch} = P_{n,t}^{G2V} + P_{n,t}^{V2V,inc} + P_{n,t}^{PV}, \quad \forall n, t \in (T_n^a, T_n^d] \tag{3.8}$$

Equation (3.9) denotes that the discharging power of each EV at time $t$ ($P_{n,t}^{EV,dsch}$) equals to the sum of the power injected to the grid and other EVs.

$$P_{n,t}^{EV,dsch} = P_{n,t}^{V2G} + P_{n,t}^{V2V,out}, \quad \forall n, t \in (T_n^a, T_n^d] \tag{3.9}$$

Thanks to (3.10) and (3.11), it is not possible for EVs to charge and discharge at the same time.

$$P_{n,t}^{EV,ch} \leq N * (1 - u_{n,t}^1), \quad \forall n, t \in (T_n^a, T_n^d] \tag{3.10}$$

$$P_{n,t}^{EV,dsch} \leq N * u_{n,t}^1, \quad \forall n, t \in (T_n^a, T_n^d] \tag{3.11}$$

### 3.1.3 Constraints and Equations of Electric Vehicle Parking Lot

Equation (3.12) states that the total power drawn by the EVs from the PV at time $t$ is equal to the PV production at time $t$.

$$P_t^{PV,forecast} = \sum P_{n,t}^{PV}, \quad \forall t \tag{3.12}$$

The total power drawn from the grid is equal to the sum of the power drawn by each EV $n$ from the grid at each time $t$ as expressed in (3.13). If the system operator sets a power limit for the parking lot, the total power drawn from the grid is limited by (3.14).

$$P_t^{G2V,total} = \sum P_{n,t}^{G2V}, \quad \forall t \tag{3.13}$$

$$P_t^{G2V,total} \leq P_t^{PLL,signal}, \quad \forall t \tag{3.14}$$

The total power injected to the grid from the parking lot is equal to the sum of the power injected by each EV $n$ ($P_{n,t}^{V2G}$) to the grid as stated in (3.15). The power injected to the grid from the parking lot at each time $t$ is determined by a contract with the DSO. Equation (3.16) ensures that the agreed power is injected to the grid at each time $t$.

$$P_t^{V2G,total} = \sum P_{n,t}^{V2G}, \quad \forall t \tag{3.15}$$

$$P_t^{V2G,total} = P_t^{V2G,contract}, \quad \forall t \tag{3.16}$$

Thanks to (3.17) and (3.18), bidirectional power flow between grid and parking lot cannot occur at the same time. Moreover, $N$ is a sufficiently large number to balance power flow.

$$P_t^{V2G,total} \leq N * u_t^2, \quad \forall t \tag{3.17}$$

$$P_t^{G2V,total} \leq N * 1 - u_t^2, \quad \forall t \tag{3.18}$$

Equation (3.19) provides that total outgoing V2V power equals total incoming V2V power.

$$\sum P_{n,t}^{V2V,out} = \sum P_{n,t}^{V2V,inc}, \quad \forall t \tag{3.19}$$

### 3.1.4 Determining Electric Vehicle Comfort

Equation (3.20) states that the SoE ($SoE_{n,t}^{EV}$) of EV at the departure time is assumed as final SoE ($SoE_n^{EV,final}$).

$$SoE_n^{EV,final} = SoE_{n,t}^{EV}, \quad \forall n,\ if\ t = T_n^d \tag{3.20}$$

In order to ensure EV comfort, the final SoE ($SoE_n^{EV,final}$) cannot be less than the initial SoE of EV $n$ ($SoE_n^{EV,init}$) as stated in (3.21).

$$SoE_n^{EV,init} \leq SoE_{n,t}^{EV} \leq SoE_n^{EV,des}, \forall n \ , if \ \ t = T_n^d \tag{3.21}$$

It should be stated that SoE cannot exceed the desired SoE at the departure time, and (3.22) states the relationship between final SoE and desired SoE. Moreover, $SoE_n^-$ takes value if the desired SoE does not reach the final SoE, otherwise $SoE_n^+$ takes value.

$$SoE_n^{EV,final} = SoE_n^{EV,des} + SoE_n^+ - SoE_n^-, \quad \forall n \tag{3.22}$$

Owing to (3.23) and (3.25), $SoE_n^+$ and $SoE_n^-$ cannot take the value at same time.

$$SoE_n^+ \leq N * (1 - u_n^3), \quad \forall n \tag{3.23}$$

$$SoE_n^- \leq N * u_n^3, \quad \forall n \tag{3.24}$$

## 3.2 LSTM Cells

Uncertainties regarding PV generation and the time of arrival of EVs to the EVPL have been taken into account with LSTM cells, a special type of RNN. As illustrated in Figure 3.2, an LSTM cell is composed of the following components: a forget gate, an update gate, an output gate, a cell state, and a hidden state [64–66]. The forget gate takes the input values ($x^{<t>}$) and the values of previous hidden state ($h^{<t-1>}$) and determines the information that should be forgotten in previous states using the sigmoid function defined by (3.25). This gate's output is a value between 0 and 1 that indicates the information's state. Output 1 indicates that the information must be kept strictly, while output 0 indicates that it must be completely forgotten.

$$\Gamma_f = \sigma(W_f[h^{<t-1>}, x^{<t>}] + b_f) \tag{3.25}$$

The update gate determines which information should be updated in the range of 0 to 1 according to its importance by inserting the input value ($x^{<t>}$) and the previous hidden state ($h^{<t-1>}$) into the sigmoid function specified in (3.26). Equation (3.27) states that $tanh$ function determines candidate cell states ($\tilde{c}^{<t>}$) ranging from -1 to 1. These two values are then multiplied pointwise to obtain the new cell state.

$$\Gamma_u = \sigma(W_u[h^{<t-1>}, x^{<t>}] + b_u) \tag{3.26}$$

$$\tilde{c}^{<t>} = tanh(W_c[h^{<t-1>}, x^{<t>}] + b_c) \tag{3.27}$$

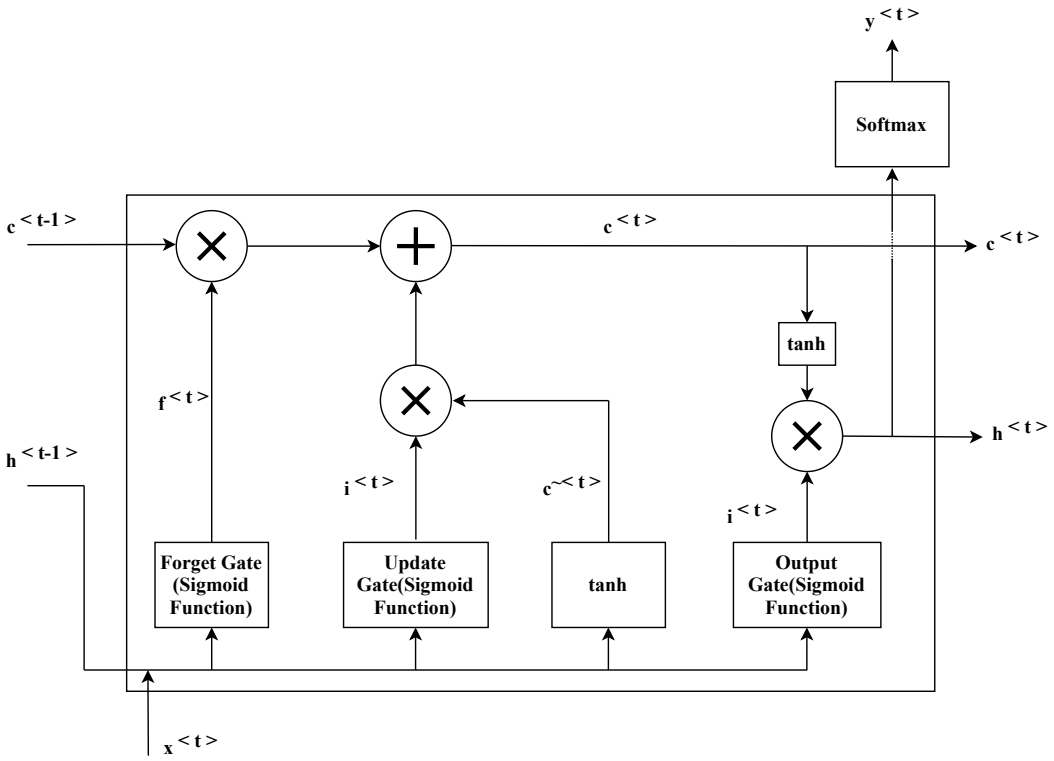



**Figure 3.2** Structure of a LSTM cell [66]

Equation (3.28) expresses that the output gate specifies what the next hidden state should be as a result of the input data and the previous hidden state.

$$\Gamma_o = \sigma(W_o[h^{<t-1>}, x^{<t>}] + b_0) \tag{3.28}$$

Equations (3.29) and (3.30) represent the variation of cell state and hidden state, respectively.

$$c^{<t>} = \Gamma_u \cdot \tilde{c}^{<t>} + \Gamma_f \cdot c^{<t-1>} \tag{3.29}$$

$$h^{<t>} = \Gamma_o * tanh(c^{<t>}) \tag{3.30}$$

# 4
# TEST AND RESULTS

A MILP model designed to minimize comfort violation of EVs is solved by taking into consideration PV and EVPL uncertainties using machine learning (ML) techniques. The proposed optimization model is developed in Python with MIP [67] library and Gurobi 9.0 [68] solver. To illustrate the computational burden, it should be noted that the solution time for all cases is less than 18 seconds with i7 6500U 2.5 GHz laptop. PV and EVPL forecasts are developed with graphics processing unit in Google Colaboratory [69] environment using ML techniques. The python codes of the designed optimization model are given in Appendix A.

## 4.1 Input Data

LSTM cells, a special type of RNN proposed by Hochreiter et al. [70] , have been widely used for time series prediction. In this study, the uncertainties associated with PV production and the arrival of EVs at the EVPL were taken into account by utilizing a machine learning algorithm based on LSTMs. The vehicles arriving at the EVPL were predicted using 4-year data from an Istanbul Metropolitan Municipality parking lot [10] , [71]. The 10-year data from National Renewable Energy Laboratory(NREL) of a point located at an approximate latitude with Istanbul was used to predict the temperature and irradiance data used in PV production [72]. Firstly, data consisting of time series with a fixed frequency are scaled in such a way that the difference between the numbers does not introduce bias and there is no vanishing gradient problem. The scaling method used in this study, the Min-Max Scaler, is defined in (4.1). Following that, the scaled data is divided into step size data and the LSTM model is used to predict.

$$X_{scaled} = \frac{X - X_{min}}{X_{max} - X_{min}} \tag{4.1}$$

Tensorflow 2.0 [73] and its Keras API [74] are used to develop the LSTM model. The input data, the LSTM model, the computational time, and the evaluation metrics as root mean square error (RMSE) for each forecasted variable are detailed in Table 4.1.

**Table 4.1** Data and model properties

| **Parameters** | **Temperature** | **Irradiance** | **Parking Lot** |
|---|---|---|---|
| Data Length | 94487 | 94487 | 132480 |
| Day | 3937 | 3937 | 1380 |
| Frequency | 1 Hour | 1 Hour | 15 minutes |
| Train/Test Size | 75540/18849 | 75516/18825 | 105695/26207 |
| Step Size | 48 | 72 | 288 |
| Input Shape | (1,48) | (1,72) | (1,288) |
| Activation Function | ReLU | ReLU | ReLU |
| Model | LSTM(300) Dense(1) | LSTM(300) Dense(1) | LSTM(300) Dense(1) |
| Optimizer | Adam | Adam | Adam |
| Loss Type | MSE | MSE | MSE |
| Final Epoch | 28 | 36 | 15 |
| Training Time | 180 s | 143 s | 105 s |
| Train RMSE | 1.270 | 78.635 | 1.696 |
| Test RMSE | 1.258 | 77.599 | 1.809 |

Figure 4.1, 4.1b and 4.1c depict the relationship between actual and prediction values for temperature, irradiance and PL and the forecasts made for 12 October. respectively.

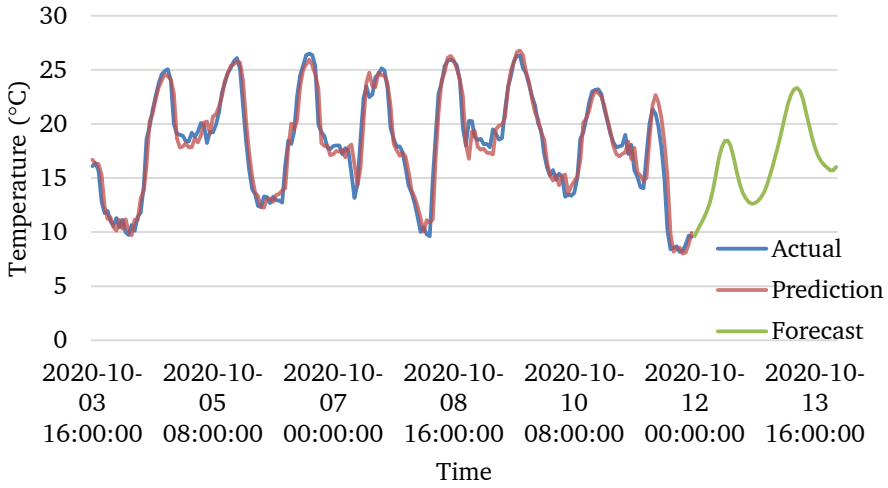
The PV plant at EVPL has a capacity of 100 kilowatt (kW). The temperature coefficient of PV plant's output power is –0.45%/°C. Equations (4.2) , (4.3) express the variation of the PV plant's output power as a function of forecasted temperature and irradiance. Temperature and irradiance Standard Test Conditions (STC) values are 25°C and 1000 $W/m^2$, respectively. Figure 4.2 demonstrates forecasted PV production.

$$P_{max@T} = \frac{(T-25) * Temp\ Coeff + 100}{100} * P_{max@25C} \tag{4.2}$$

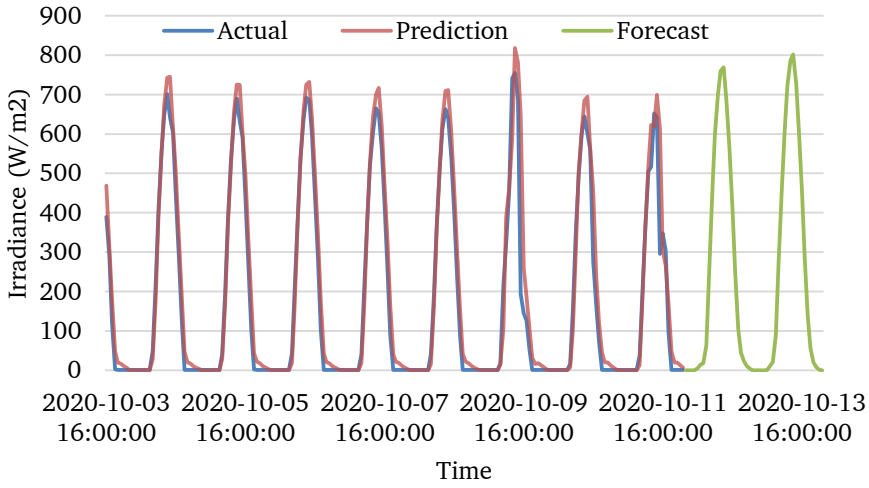
$$P_{actual@T} = \frac{Irradiance_{act}}{Irradiance_{ref}} * P_{max@T} \tag{4.3}$$

The applied ML model forecasted that 253 EVs will arrive at EVPL during the day. The EVs' departure time from EVPL and their initial SoE values are generated randomly using a truncated normal distribution via the Python Scipy library [75]. Thanks to (4.4) and command (4.5), data with a size of $N$ were randomly generated with the mean $\mu$ and standard deviation $\sigma$ between certain lower and upper bounds. Lower = 0.2, upper = 0.95, $\mu = 0.4$, $\sigma = 0.2$, N = 253 were used as initial SoE data generation parameters.

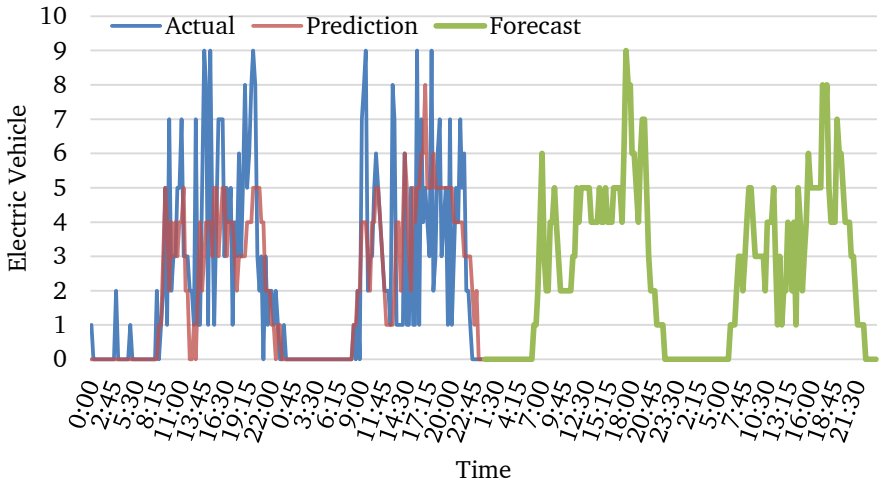
$$a, b = \frac{lower - \mu}{\sigma}, \frac{upper - \mu}{\sigma} \tag{4.4}$$




**(a)** Temperature




**(b)** Irradiance




**(c)** EVPL

**Figure 4.1** Comparison of the outputs of the ML model with actual values for temperature, irradiance and EVPL

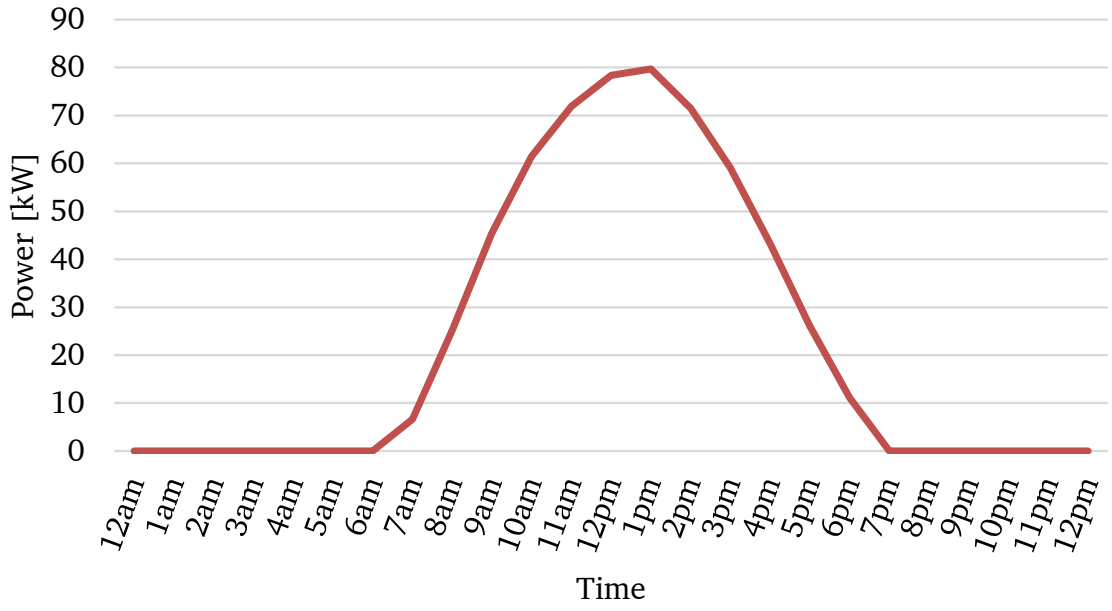



**Figure 4.2** Forecasted output power of PV

$$scipy.stats.truncnorm.rvs(a, b, loc = \mu, scale = \sigma, size = N) \tag{4.5}$$

The desired SoE parameters were randomly selected from a range of values between the initial SoE + 0.01 and the battery capacity of each EV, with a uniform distribution. Using the Python Pandas library [76], [77] , the October information of the parking data was analyzed and the statistics in Table 4.2 were obtained. The statistics obtained made it possible to generate randomized data for each hour.

Figure 4.3 illustrates the relationship between the initial SoE and the desired SoE of all EVs. To improve the accuracy of the tests, ten different types of EVs with the specifications listed in Table 4.3 were used.

## 4.2 Case Studies

Ten distinct cases were conducted to examine the proposed model and to explicitly demonstrate the effects of V2G, V2V, PLL, and PV. Developed cases are as follows:

- *Base Case-1*: No PLL signal is imposed by the system operator. V2G, V2V energy exchange and the PV system are disabled.
- *Base Case-2*: PLL signal is imposed by the system operator. Peak load is limited to 300 kW between 8 am to 11 am and 7 pm to 9 pm. V2G, V2V energy exchange and the PV system are disabled.

**Table 4.2** Statistics of the EVPL in october

| Hour | Mean [min] | Standard Deviation [min] | Minimum [min] | 25% [min] | 50% [min] | 75% [min] | Maximum [min] |
|---|---|---|---|---|---|---|---|
| 0 | 353.4211 | 265.9401 | 6 | 172.5 | 315 | 531.5 | 914 |
| 1 | 524.7778 | 267.7068 | 15 | 498 | 551 | 677 | 857 |
| 2 | 437 | 325.3148 | 10 | 152.25 | 524.5 | 649.75 | 857 |
| 3 | 498.6667 | 474.0352 | 28 | 260 | 492 | 734 | 976 |
| 4 | 59 | - | 59 | 59 | 59 | 59 | 59 |
| 5 | 680.6122 | 183.6492 | 6 | 630 | 700 | 738 | 998 |
| 6 | 661.5342 | 169.2555 | 16 | 594 | 697 | 762 | 979 |
| 7 | 646.9304 | 157.7044 | 7 | 596 | 670 | 731 | 996 |
| 8 | 603.6712 | 162.4565 | 6 | 566 | 631 | 683 | 999 |
| 9 | 513.1891 | 184.7596 | 6 | 404 | 555 | 631 | 990 |
| 10 | 413.644 | 183.6236 | 6 | 271 | 436 | 544 | 998 |
| 11 | 354.3892 | 170.9819 | 6 | 231.5 | 344 | 467 | 936 |
| 12 | 303.3294 | 153.2768 | 6 | 193 | 281 | 394 | 903 |
| 13 | 276.0478 | 142.7501 | 6 | 174 | 260 | 352.25 | 913 |
| 14 | 257.8107 | 139.9593 | 6 | 160 | 231 | 327 | 914 |
| 15 | 243.9225 | 133.0149 | 6 | 150 | 217 | 307 | 994 |
| 16 | 264.8508 | 160.4683 | 6 | 161 | 232 | 340 | 992 |
| 17 | 287.6532 | 173.9321 | 6 | 182 | 267 | 343 | 993 |
| 18 | 289.106 | 182.8925 | 6 | 195 | 252 | 319 | 991 |
| 19 | 273.3579 | 185.7203 | 6 | 179 | 242 | 297 | 986 |
| 20 | 263.4701 | 217.4379 | 6 | 144 | 225.5 | 271.75 | 996 |
| 21 | 319.5986 | 230.2582 | 6 | 167.25 | 203 | 554 | 931 |
| 22 | 310.1011 | 287.4558 | 6 | 33 | 156 | 603 | 934 |
| 23 | 385.8378 | 349.7932 | 6 | 45 | 304 | 699 | 950 |

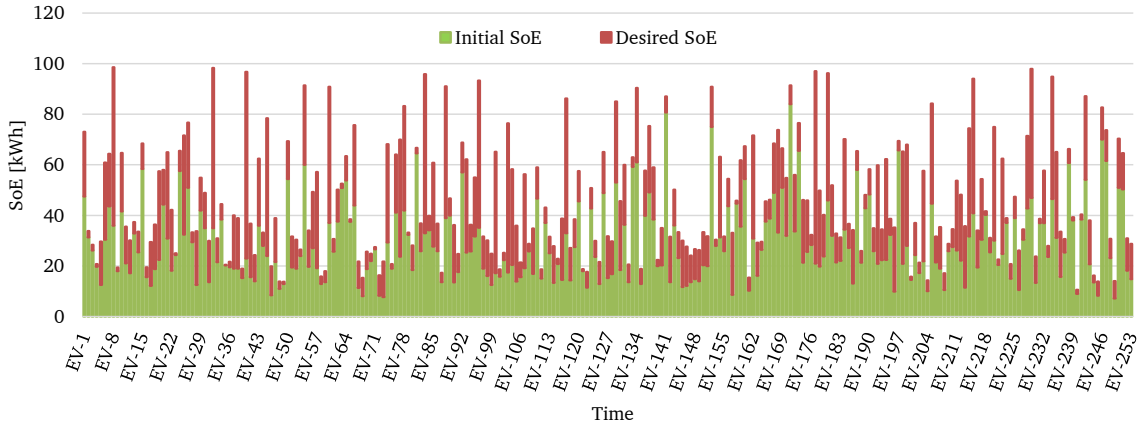



**Figure 4.3** Comparison of initial SoE and desired SoE of each EV

**Table 4.3** Specifications of EVs that used in case studies

| **EV Types** | **Battery Capacity [kWh]** | **Charging Rate [kW]** |
|---|---|---|
| Audi e-Tron [78] | 95 | 11 |
| BMW i3 [79] | 42.2 | 11 |
| Tesla Model X [80] | 100 | 17.2 |
| Chevrolet Bolt [81] | 66 | 7.2 |
| Mercedes EQC [82] | 80 | 7.4 |
| Hyundai Kona [83] | 39.2 | 7.2 |
| Volkswagen Golf [84] | 35.8 | 7.2 |
| KIA Soul 39 [85] | 39.2 | 7.2 |
| Porsche Taycan 4S [86] | 79.2 | 11 |
| Seat Mii [87] | 36.8 | 7.2 |

- *Case-1*: No PLL signal is imposed by the system operator. V2V energy exchange and the PV system are disabled.
- *Case-2*: PLL signal is imposed by the system operator. Peak load is limited to 300 kW between 8 am to 11 am and 7 pm to 9 pm. V2V energy exchange and PV system are disabled.
- *Case-3*: No PLL signal is imposed by the system operator. V2V energy exchange is enabled and the PV system is disabled.
- *Case-4*: PLL signal is imposed by the system operator. Peak load is limited to 300 kW between 8 am to 11 am and 7 pm to 9 pm. V2V energy exchange is enabled and the PV system is disabled.
- *Case-5*: No PLL signal is imposed by the system operator. V2V energy exchange is disabled and the PV system is enabled.
- *Case-6*: PLL signal is imposed by the system operator. Peak load is limited to 300 kW between 8 am to 11 am and 7 pm to 9 pm. V2V energy exchange is disabled and the PV system is enabled.
- *Case-7*: No PLL signal is imposed by the system operator. V2V energy exchange and the PV system are enabled.
- *Case-8*: PLL signal is imposed by the system operator. Peak load is limited to 300 kW between 8 am to 11 am and 7 pm to 9 pm. V2V energy exchange and the PV system are enabled.

Table 4.4 summarizes the case studies for ease of examination.

**Table 4.4** Comparisons of the case studies

| | Base Case-1 | Base Case-2 | Case-1 | Case-2 | Case-3 | Case-4 | Case-5 | Case-6 | Case-7 | Case-8 |
|---|---|---|---|---|---|---|---|---|---|---|
| V2G | - | - | ✓ | ✓ | ✓ | ✓ | ✓ | ✓ | ✓ | ✓ |
| PLL | - | ✓ | - | ✓ | - | ✓ | - | ✓ | - | ✓ |
| V2V | - | - | - | - | ✓ | ✓ | - | - | ✓ | ✓ |
| PV | - | - | - | - | - | - | ✓ | ✓ | ✓ | ✓ |

## 4.3 EVPL Power Variations

This section examines the optimal operation of EVPL in terms of power changes in the absence of V2G and V2V applications. Following that, the variations between all case studies and these two base cases are identified, and the case studies are compared to one another.

Figure 4.4 illustrates the variation in the amount of power drawn from the grid by EVPL in *Base Case-1* and *Base Case-2*. When PLL, V2G, and V2V are not active, EVPL operates solely as a load in *Base Case- 1*, and the effect of PLL on this situation is investigated in *Base Case-2*. As illustrated in Figure 4.4, PLL is successfully utilized between the hours of 8 am and 11 am and 7 pm and 9 pm. This situation, however, results in the emergence of new peak powers.

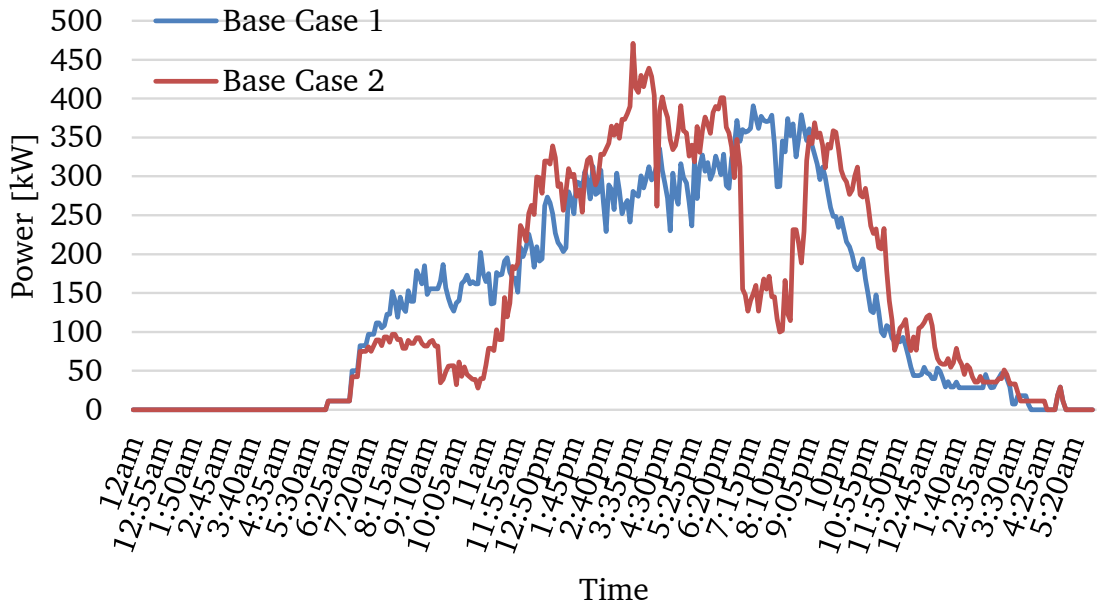



**Figure 4.4** Power drawn from grid in Base Case-1 and Base Case-2

The effect of V2G on the power change in EVPL is examined in Figure 4.5. In comparison to *Base Case-1* and *Base Case-2*, the V2G process increases the amount of power drawn from the grid by EVPL. Power drawn from the grid is shifted to off-peak hours in the absence of PLL and V2G operations. Between 1.45 and 5.25 p.m. in *Case-2*, the PLL causes the EVPL to reach its maximum power demand.

Figure 4.6 illustrates the effect of V2V, V2G, and PLL operation cooperation on EVPL power variation. When the V2V operation is activated, it significantly increases the amount of power that EVPL draws from the grid. In *Case-4*, the EVPL's power consumption is limited by the PLL signal during the hours when the PLL procedure is being used. However, this situation forces the EVPL to operate at maximum capacity for an extended period of time during V2G and non-PLL hours. Although there is no PLL in *Case-3*, high power draws occur due to V2V. Thus, it is critical for both the DSO and the EVPL operator to manage peak loads caused by V2V and PLL operation.

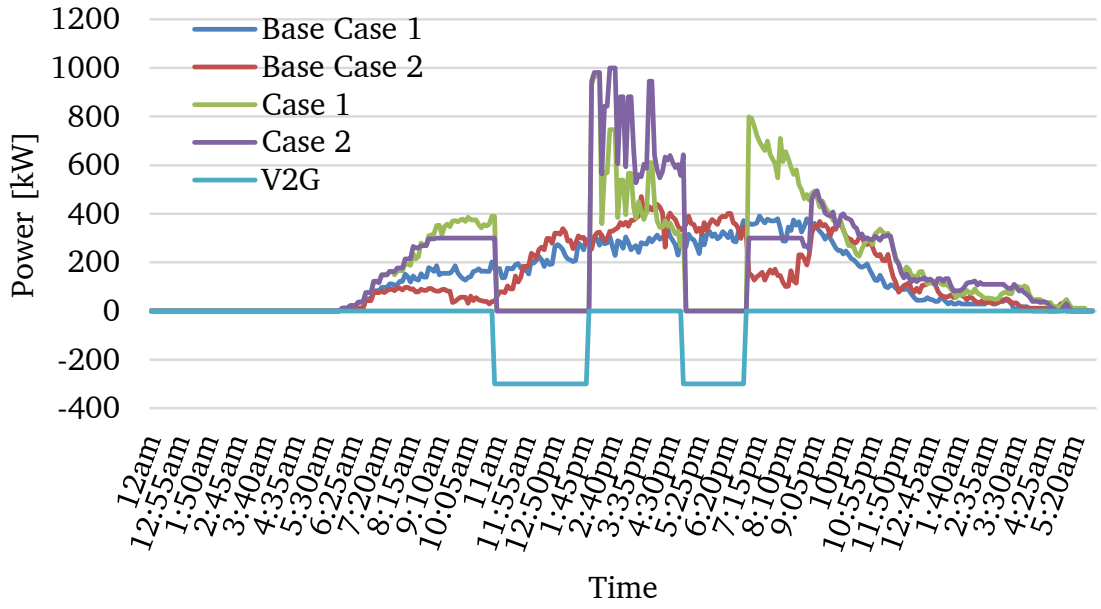



**Figure 4.5** Comparison of the power drawn from grid in Case-1 and Case-2 with Base Case-1 and Base Case-2

The effects of PV generation and V2G operation on EVPL power consumption are depicted in Figure 4.7 . In *Case-1* and *Case-2*, Prior to 11 a.m., PV production enables a power consumption comparable to *Base Case-1*. It is observed that the hours without V2G and PLL consume more power than the base cases. This consumption, however, does not reach the station's maximum power output. PV generation mitigates the EVPL power system's V2G and PLL effects.

Figure 4.8 depicts the effects of V2G, PLL, V2V, and PV cooperation on EVPL's power consumption. New peak powers appear in hours that do not include V2V and V2G, V2G and PLL, unlike *Base Case-1* and *Base Case-2*. PV generation, on the other hand, prevents the station from operating at full capacity.

Figure 4.9 illustrates the amount of power drawn from and injected into the grid in each case study. The results indicate that the PLL application is effective at limiting peak load during the specified hours. The hours during which power is drawn from

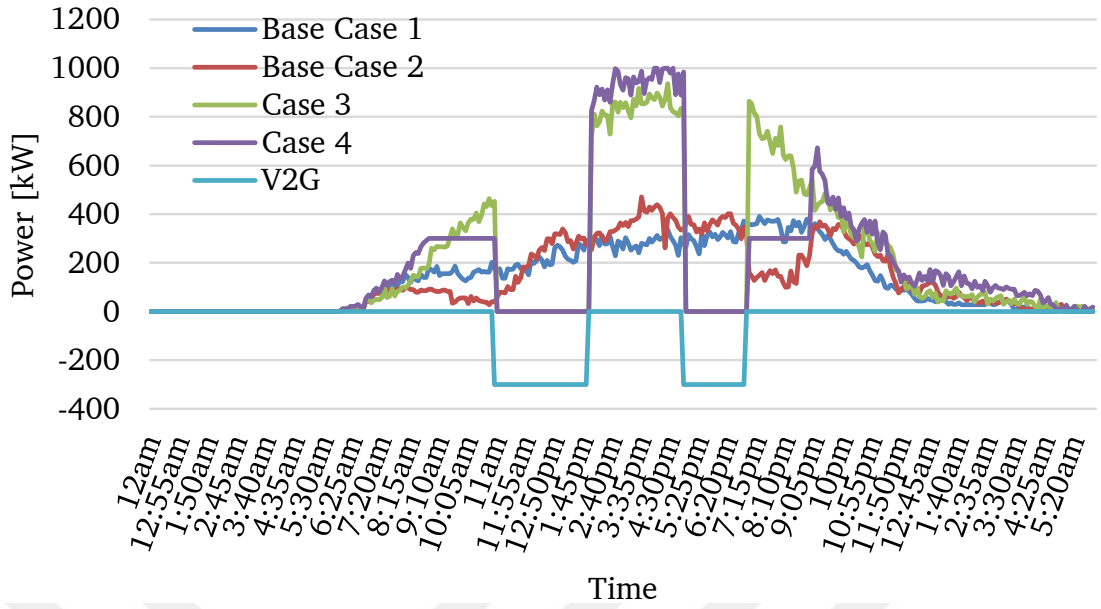



**Figure 4.6** Comparison of the power drawn from grid in Case-3 and Case-4 with Base Case-1 and Base Case-2

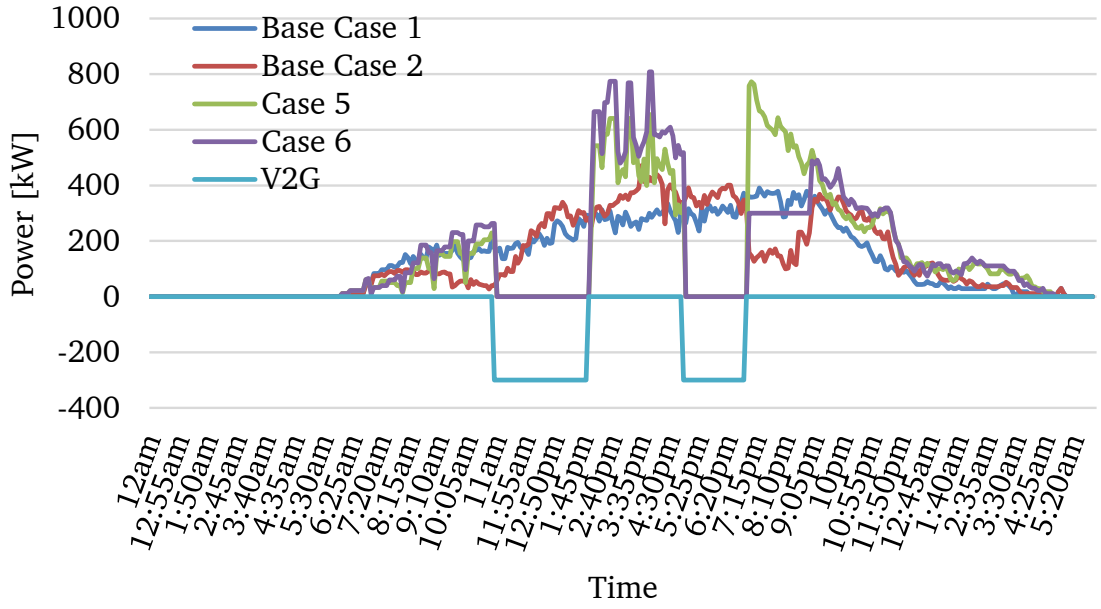



**Figure 4.7** Comparison of the power drawn from grid in Case-5 and Case-6 with Base Case-1 and Base Case-2

the grid are shifted to those when V2G and PLL activity are not present. When non-PV case studies are analyzed, it is discovered that PLL operation results in the creation of new peak load points. EVPL operates at maximum load for a longer period of time in *Case-4*, where both V2V and PLL modes are active than in the other cases. When case studies involving active PV production are analyzed, it is observed that the peaks caused by PLL application are significantly reduced. In contrast to *Case-4*, the EVPL does not operate at full load in *Case-8*, owing to the presence of PV generation.

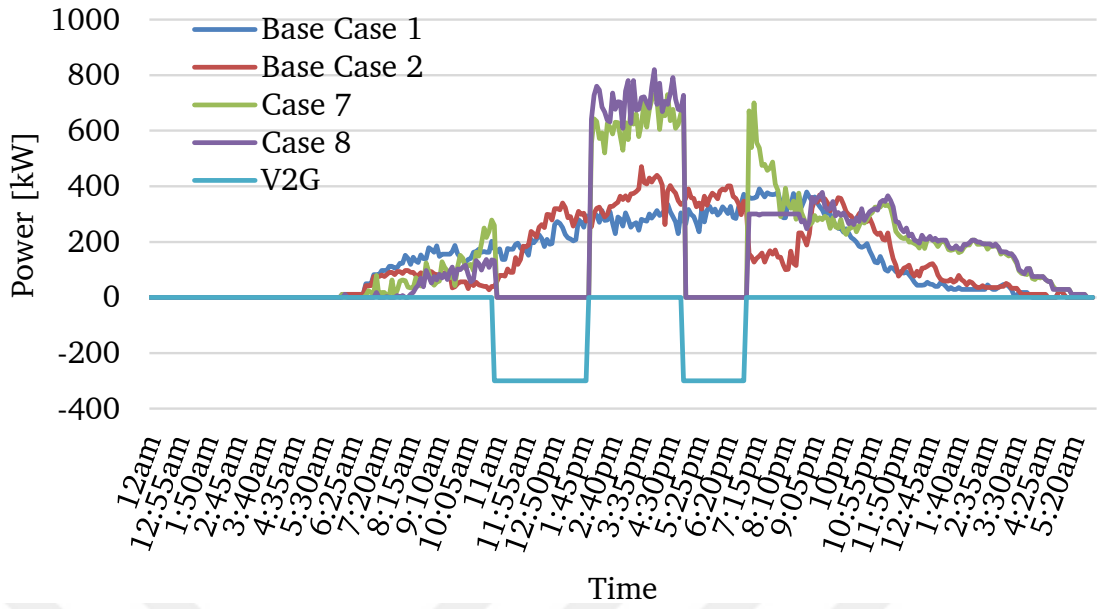



**Figure 4.8** Comparison of the power drawn from grid in Case-7 and Case-8 with Base Case-1 and Base Case-2

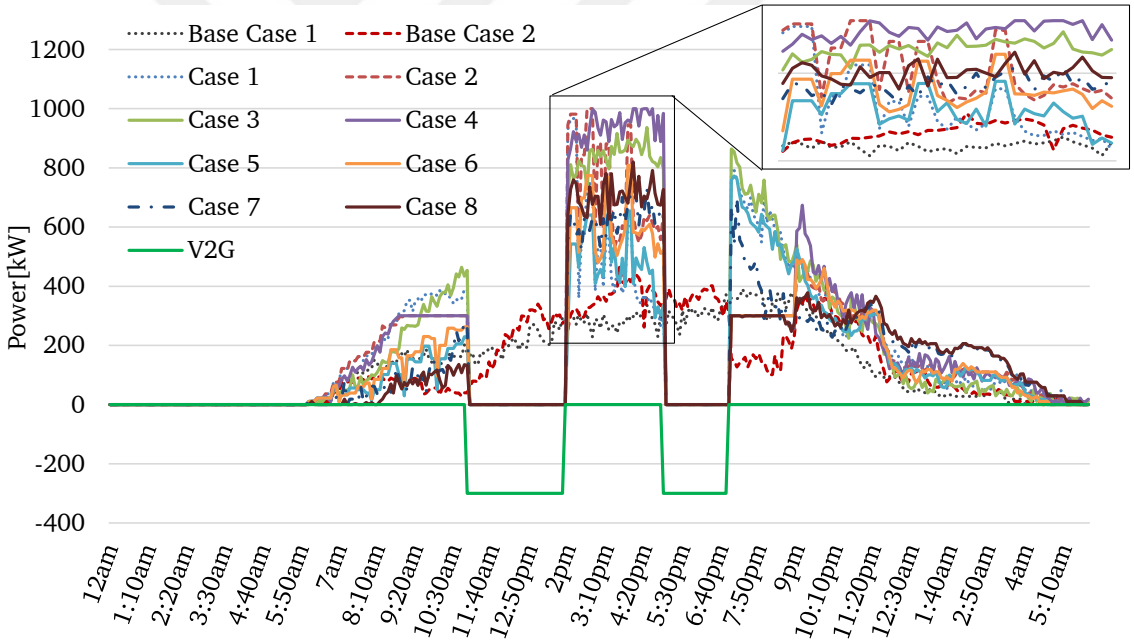



**Figure 4.9** Power drawn from grid and power injected into the grid for all case studies.

Figure 4.10 illustrates the variation in V2V along with all case studies. In *Case-3* and *Case-4*, energy transfer between EVs is quite more during V2G activity hours. Excluding evenings when there is no PV production, *Case-7* and *Case-8* contain fewer V2V operations than *Case-3* and *Case-4*. Due to their desire to reach their required level of charge, it is observed that EVs are less likely to participate in the V2V process before the hours that contain PLL.

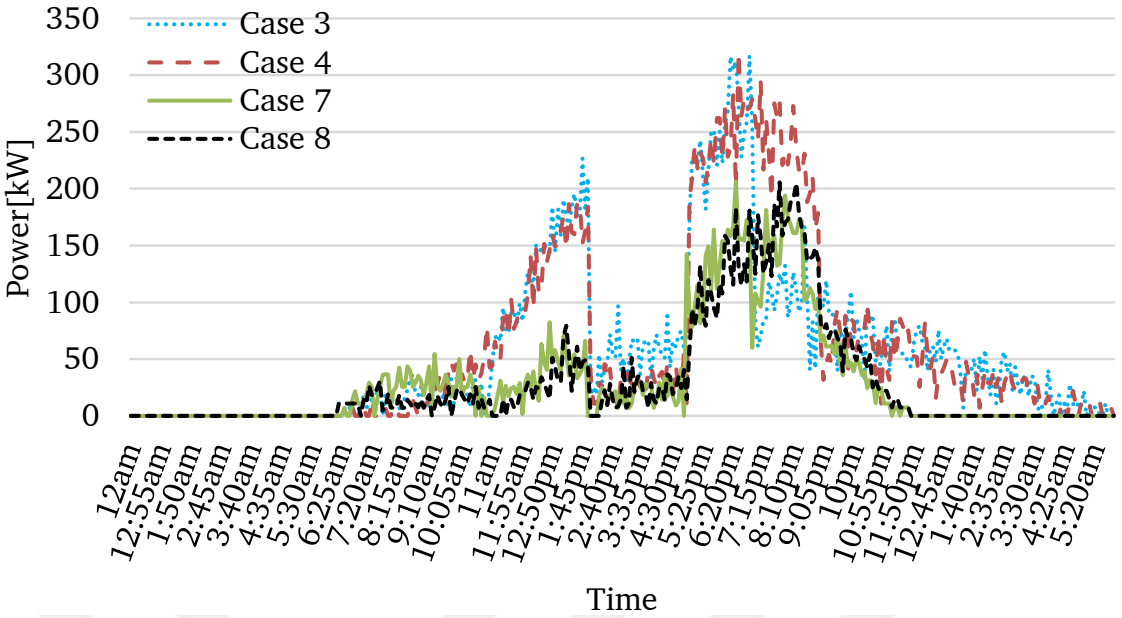



**Figure 4.10** V2V power variations

**Table 4.5** Comparison of the results of EVPL for evaluated case studies

| Case Studies | Comfort Violation | G2V Energy [kWh] | Load Factor [%] | V2V Energy [kWh] | Charging Energy [kWh] | Discharging Energy [kWh] |
|---|---|---|---|---|---|---|
| Base Case-1 | 2.23 | 4138.720 | 35.32 | - | 4138.770 | 0 |
| Base Case-2 | 2.23 | 4132.639 | 29.26 | - | 4132.639 | 0 |
| Case-1 | 4.82 | 5300.526 | 18.28 | - | 5300.526 | 1499.4 |
| Case-2 | 4.82 | 5300.526 | 17.68 | - | 5300.526 | 1499.4 |
| Case-3 | 2.23 | 6037.188 | 21.49 | 1723.887 | 7761.075 | 3223.287 |
| Case-4 | 2.23 | 6011.110 | 20.05 | 1816.052 | 7827.162 | 3315.452 |
| Case-5 | 2.99 | 4454.390 | 19.22 | - | 5613.586 | 1499.4 |
| Case-6 | 2.99 | 4468.765 | 18.44 | - | 5627.961 | 1499.4 |
| Case-7 | 2.23 | 4679.879 | 21.36 | 909.412 | 6748.486 | 2408.812 |
| Case-8 | 2.23 | 4676.647 | 19.02 | 879.494 | 6415.336 | 2378.894 |

The results of case studies are compared in Table 4.5. It is worth noting that the PLL does not result in a violation of comfort. The load factor decreases as a result of the new peaks in PLL operation. V2V improves comfort in all of these cases. In *Case-3* and *Case-4*, power drawn from the grid increases as a result of V2V operation. In *Case-4*, since sufficient power from the grid could not be drawn due to the PLL, the V2V increases, and the EVs are discharged more. In scenarios involving PV energy, the amount of power drawn from the grid is decreased. In *Case-7* and *Case 8*, the vehicles are less discharged and fewer V2V transactions occur than in *Case-3* and *Case-4*. In *Case-8*, since the EVs can not be charged enough to participate in the V2V activity in the morning due to PLL, optimization is made to take power from the PV during the peak hours of V2G and PLL activity. Consequently, contrary to *Case-4*, the PLL reduces the number of V2V operations. Since vehicles can be charged from PV during the hours of PLL and V2V operations, less V2V is required compared to *Case-3* and *Case-4*.

## 4.4 SoE and Power Variations of EVs

In this section, the power and energy variations of electric vehicles with different parking times are examined.

### 4.4.1 SoE and Power Variations of the EV - 103

In this subsection, the power and energy variations of an EV that is present in the EVPL between 1.30 pm and 8.20 pm and whose energy demand is 58.946 kWh are shown. Figure 4.11 shows that EV reaches the desired SoE level without any comfort violation

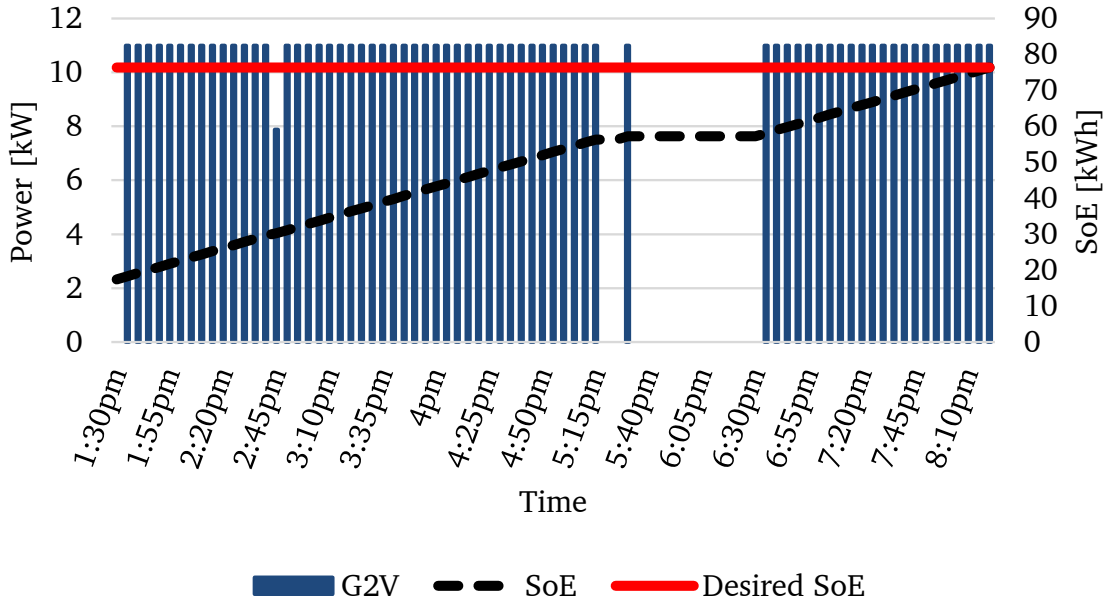



**Figure 4.11** SoE and power variations of EV-103 (Base Case-1)

Figure 4.12 demonstrates the effect of PLL on EV charging process in *Base Case-2*. Due to the PLL operation between 7 pm and 9 pm, the charging process of the vehicle is shifted to the hours preceding the PLL, in contrast to the EV's charging pattern in *Base Case-1*. This does not, however, compromise the EV's comfort.

The energy and power changes of the EV in *Case-1* and *Case-2* are depicted in Figure 4.13. V2G transactions occur between the hours of 5 p.m and 7 p.m at EVPL. The EV can not draw power from the grid because the power transfer from the EVPL to the grid and the grid to the EVPL can not occur simultaneously. As a result, the EV's comfort is compromised. Additionally, PLL operation in *Case-2* has no effect on the EV's charging pattern. The PLL process does not involve EVs whose energy requirements can not be met.

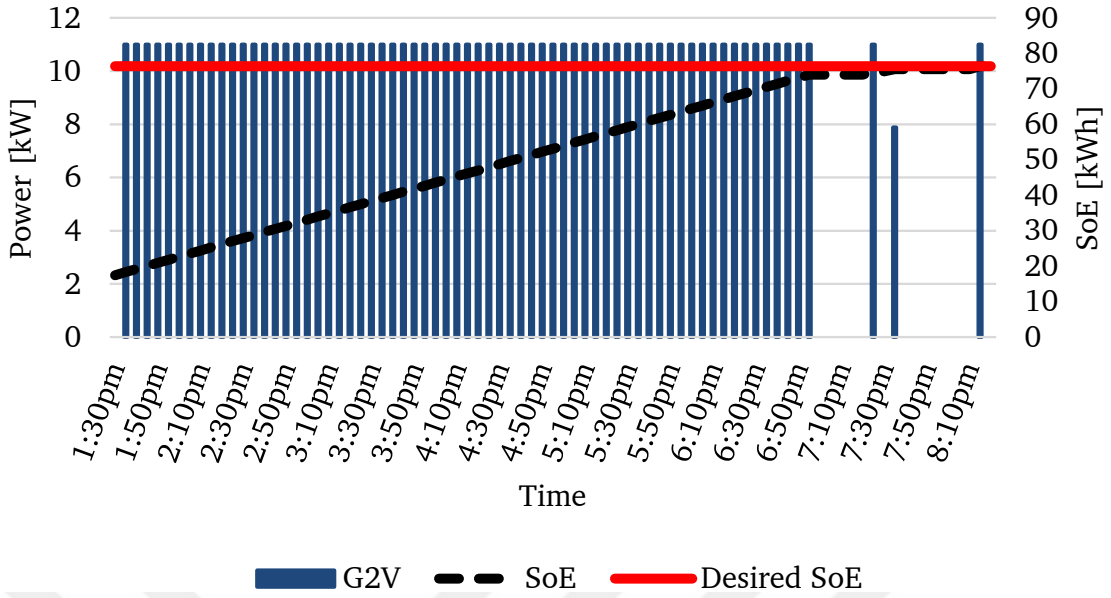



**Figure 4.12** SoE and power variations of EV-103 (Base Case-2)

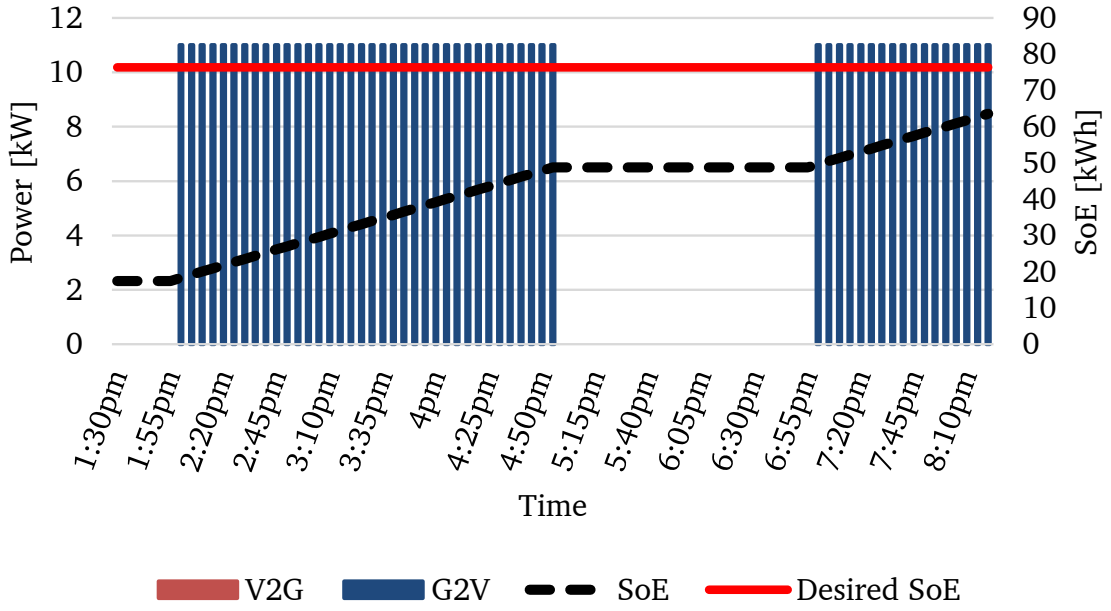



**Figure 4.13** SoE and power variations of EV-103 (Case-1 and Case-2)

Figure 4.14 illustrates the effect of V2V operation on the power and energy consumption of the EV in *Case-3*. In *Cases-1 and 2*, it is demonstrated that the EV that is unable to reach the desired SoE level due to V2G reaches it by drawing power from other EVs. Aside from eliminating the EV's comfort violation, the EV is seen to assist other EVs in minimizing comfort violations by injecting power to other EVs when necessary.

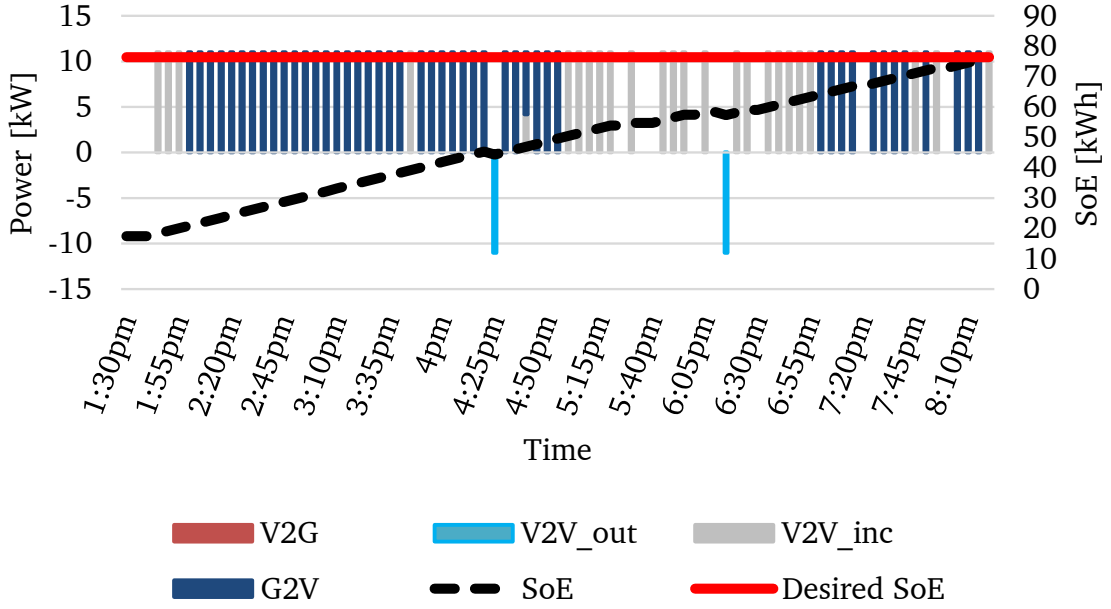



**Figure 4.14** SoE and power variations of EV-103 (Case-3)

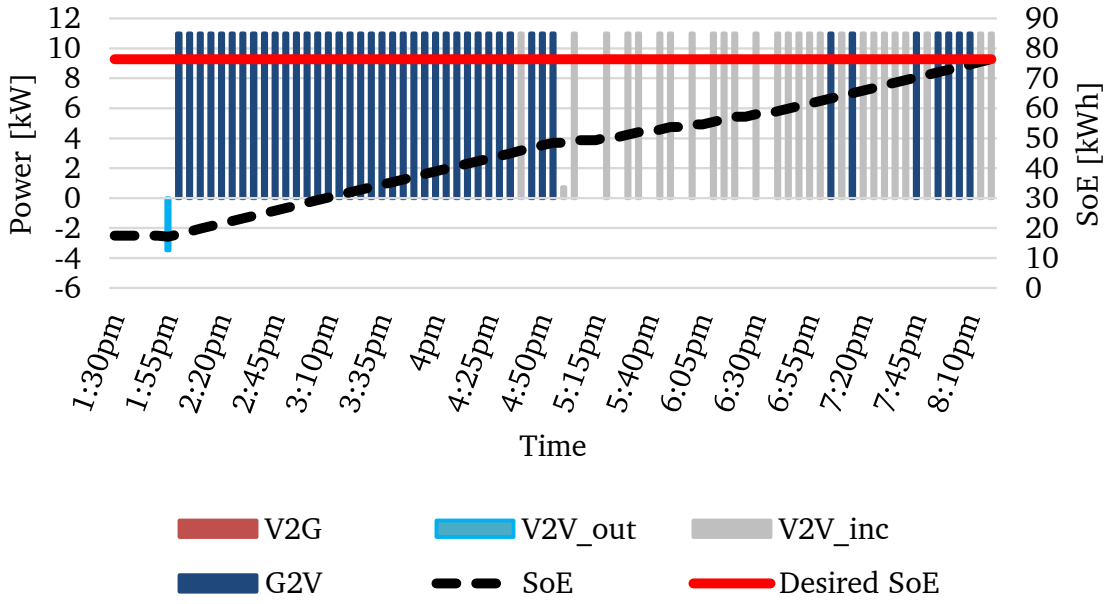



**Figure 4.15** SoE and power variations of EV-103 (Case-4)

Figure 4.15 illustrates the effect of V2V and PLL on the EV's power and energy consumption in *Case-4*. Despite the fact that PLL is enabled, the EV does not experience comfort violations as a result of drawing power from other vehicles thanks to the V2V. Due to PLL, the EV, however, injects less power into other EVs than in *Case-3*.

Figure 4.16 illustrates the effect of V2G and PV generation on EV power and energy exchange in *Case-5*. While the EV can not reach the desired SoE level, it can be able

to charge more than in *Cases-1 and 2*, owing to the PV generation. Between 5 pm and 7 pm, when power can not be drawn from the grid due to V2G, the EV's comfort is provided by drawing power from the PV.

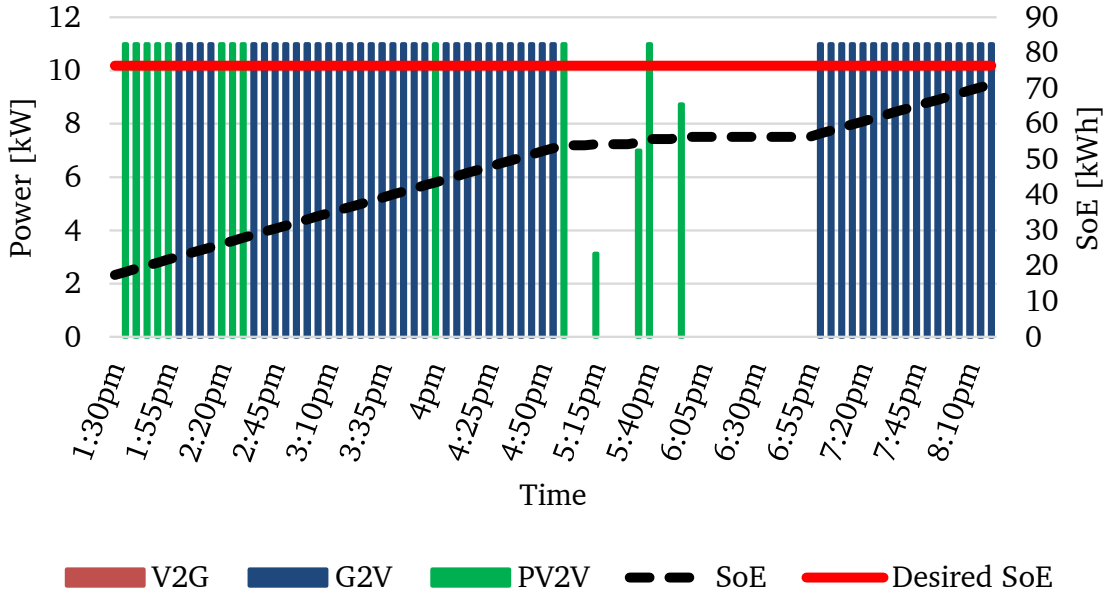



**Figure 4.16** SoE and power variations of EV-103 (Case-5)

Figure 4.17 examines the effect of V2V, V2G, and PV operation on the EV's power and energy variations. In comparison to *Case-3*, which does not include PV generation, it is obvious that PV eliminates the need for power transfer to other EVs. Additionally, when compared to other case studies, the EV's participation in V2V is reduced, but there is no violation of comfort. Therefore , PV generation is critical to EVPL's operation.

In figure 4.18, the effect of V2V, V2G, PLL and PV combined operation on EV power and energy change is examined. Along with resolving the vehicle's comfort violation via V2V, *Case-8* demonstrates that the vehicle participates in the V2G operation and provides ancillary services to the distribution network.

Table 4.6 summarizes the results for the EV-103 that is parked in the EVPL. When the results are analyzed in terms of comfort violation, it is evident that the comfort of EV is compromised in the absence of V2V due to V2G operation. While PV generation mitigates the violation of comfort in *Cases-5 and 6*, EV can not reach the desired SoE level without V2V transaction.As can be seen, V2V is critical in preventing discomfort. Moreover, in addition to providing relevant EV comfort, it also increases the comfort of other EVs by participating in the V2V transactions. The comfort of the relevant EV is provided by fewer V2V transactions in *Case-7* and *Case-8* than *Case-3* and *Case-4*

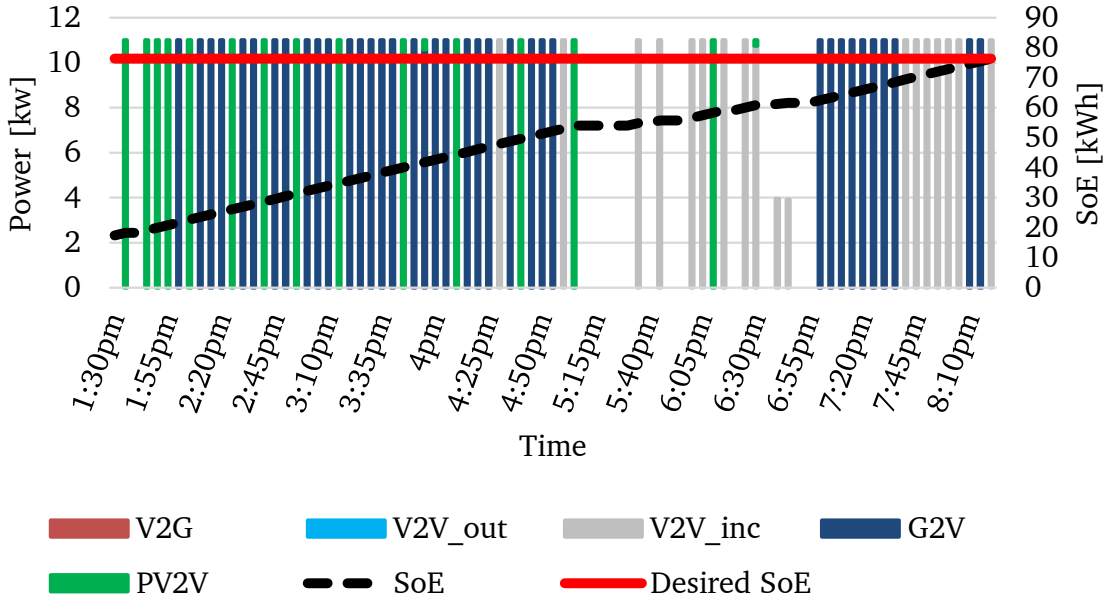



**Figure 4.17** SoE and power variations of EV-103 (Case-7)

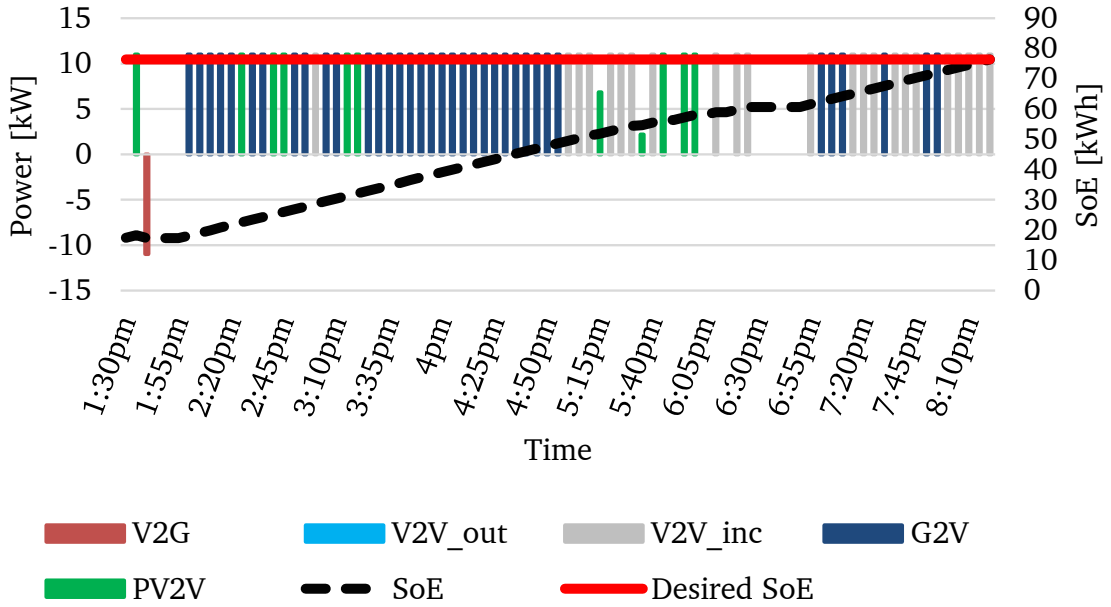



**Figure 4.18** SoE and power variations of EV-103 (Case-8)

due to PV production. It is seen that the EV, which is provided with comfort in Case 8, also participates in the V2G event. Thus, in addition to ensuring the comfort of the EV thanks to V2V and PV, it is ensured that this EV is later included in V2G and V2V transactions.

**Table 4.6** Comparison of the results of EV-103 in evaluated case studies

| Case Studies | G2V [kWh] | V2V_inc [kWh] | V2V_out [kWh] | PV2V [kWh] | V2G [kWh] | Final SoE [kWh] | Desired SoE [kWh] | Comfort Violation[%] |
|---|---|---|---|---|---|---|---|---|
| Base Case 1 | 62.048 | - | - | - | - | 76.37 | 76.37 | 0 |
| Base Case 2 | 62.048 | - | - | - | - | 76.37 | 76.37 | 0 |
| Case 1 | 48.564 | - | - | - | 0 | 63.56 | 76.37 | 16.17 |
| Case 2 | 48.564 | - | - | - | 0 | 63.56 | 76.37 | 16.17 |
| Case 3 | 41.8 | 22.279 | 1.833 | - | 0 | 76.37 | 76.37 | 0 |
| Case 4 | 38.485 | 23.885 | 0.29 | - | 0 | 76.37 | 76.37 | 0 |
| Case 5 | 44.899 | - | - | 11.651 | 0 | 71.15 | 76.37 | 6.59 |
| Case 6 | 44.899 | - | - | 12.367 | 0 | 71.83 | 76.37 | 5.73 |
| Case 7 | 33.869 | 15.296 | 0 | 12.884 | 0 | 76.37 | 76.37 | 0 |
| Case 8 | 32.987 | 21.074 | 0 | 9.002 | 0.916 | 76.37 | 76.37 | 0 |

### 4.4.2 SoE and Power Variations of the EV - 166

In this subsection, the power and energy variations of an EV that is present in the EVPL between 5 pm and 6.35 pm and whose energy demand is 7.342 kWh are shown.

The power and energy variations of the EV in *Base Case-1* are depicted in Figure 4.19. When EVPL operates solely as a load, the EV reaches the desired charge level without causing any discomfort.

The power and energy state changes of the EV in *Case-1* and *Case-2* are visualized in Figure 4.20. Because the V2G operation is active during the hours when the EV is in EVPL, the EV can not draw power from the grid. As a result, the EV can not be charged. V2G causes the inability of EVs with short parking times to meet their charging requirements.

Figure 4.21 shows the power and energy changes of the EV that can not draw power from the grid due to V2G when V2V and PLL are active in *Case-4*. The V2V process ensures that the EV reaches the desired charge level. Additionally, it contributes to the comfort of other EVs by transferring power to them. The V2V's efficacy in enhancing the overall comfort of EVs in EVPL is clearly evident.

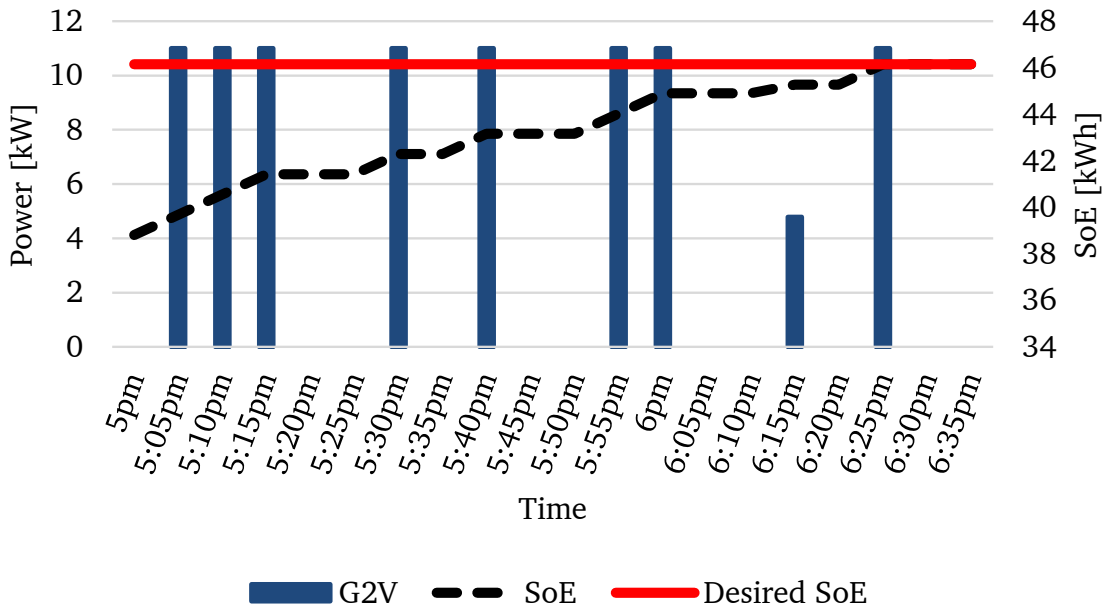



**Figure 4.19** SoE and power variations of EV-166 (Base Case-1)

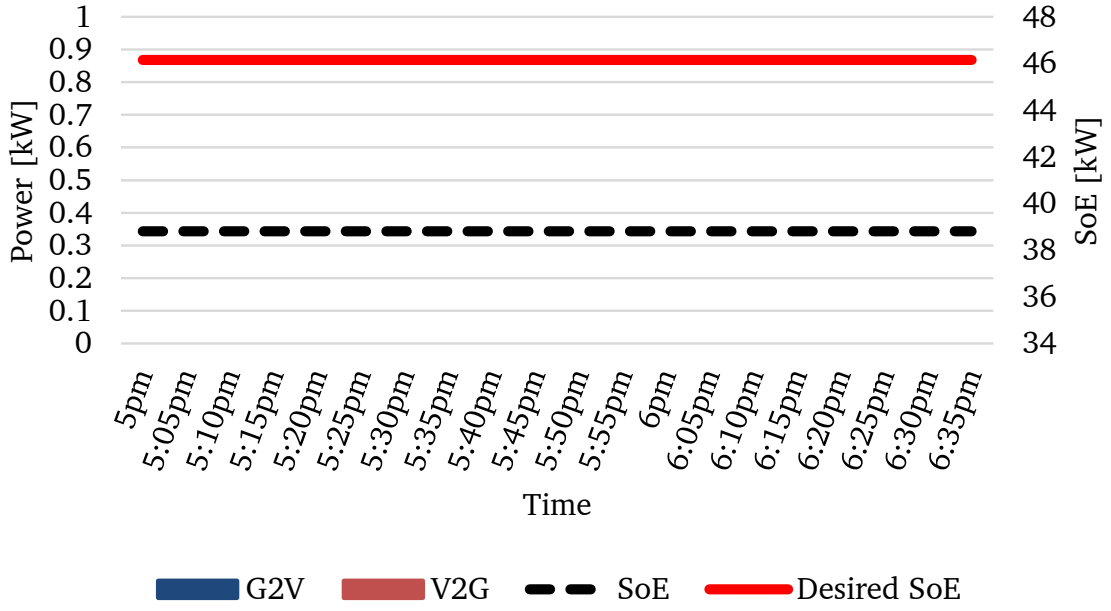



**Figure 4.20** SoE and power variations of EV-166 (Case-1 and Case-2)

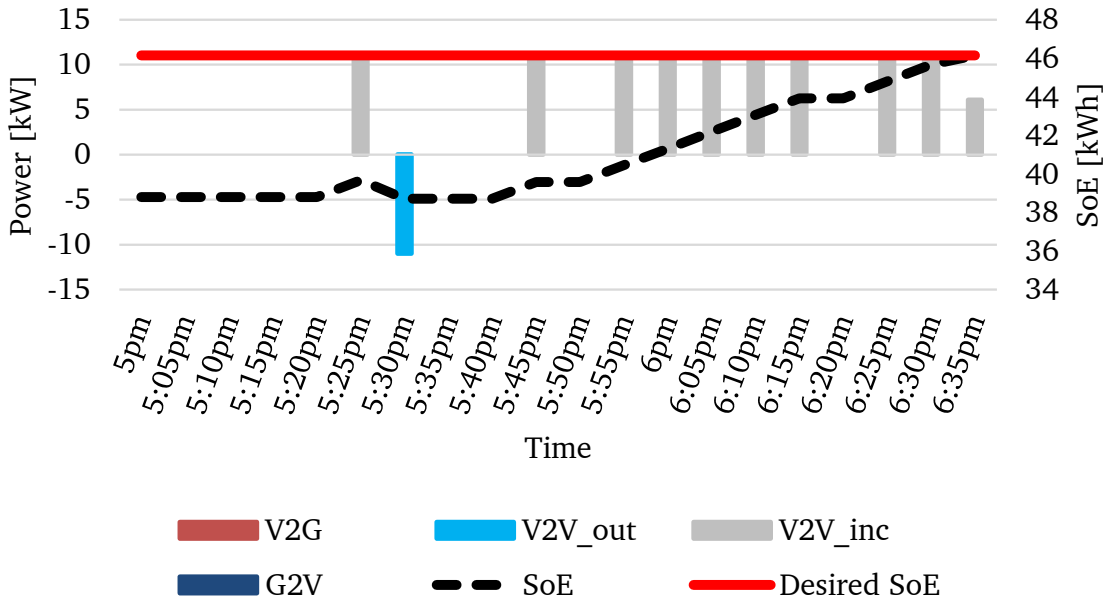



**Figure 4.21** SoE and power variations of EV-166 (Case-4)

The power and energy variations of the EV in *Case-5* are represented in Figure 4.22. Unlike in *Cases-1 and 2*, EV can be charged via PV generation. However, PV generation still cannot be sufficient and the EV can not reach the desired charge level.

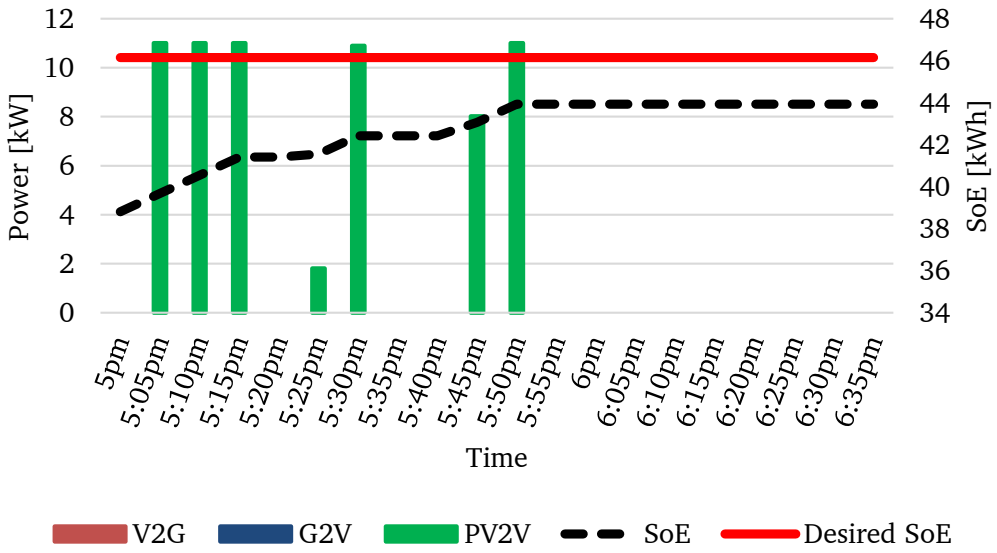



**Figure 4.22** SoE and power variations of EV-166 (Case-5)

The power and energy variations of the EV in *Case-5* are depicted in Figure 4.23. Thanks to PV and V2V, EV reaches the desired charge level. Unlike in *Case-4*, the EV does not require power transfer to other vehicles to increase overall comfort in the EVPL. PV generation's beneficial effect on increasing comfort and reducing the need for V2V is obvious.

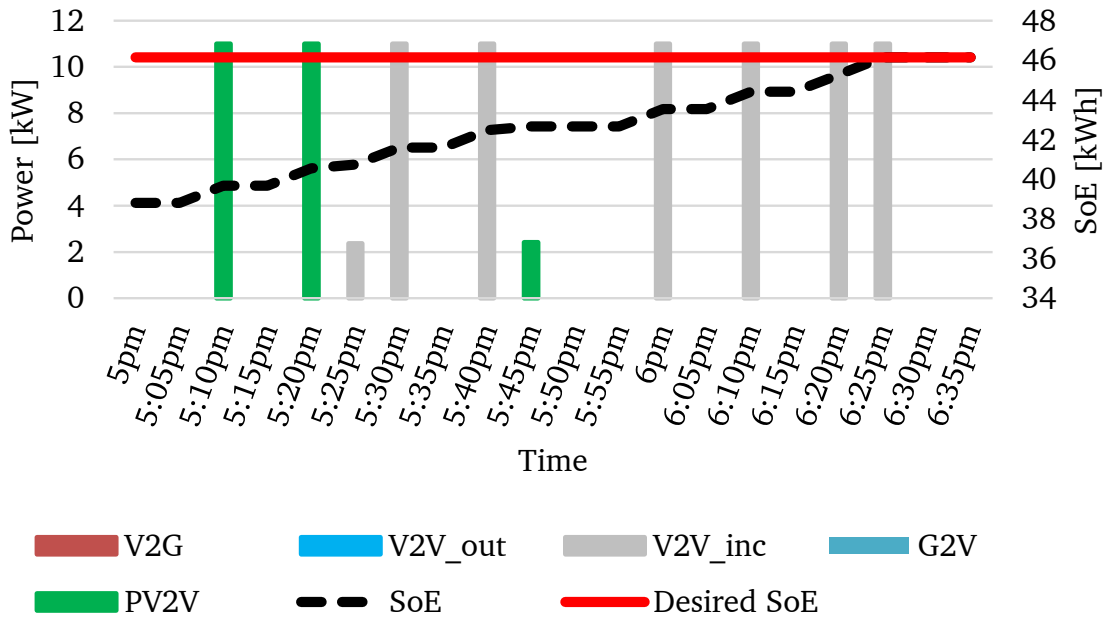



**Figure 4.23** SoE and power variations of EV-166 (Case-8)

**Table 4.7** Comparison of the results of EV-166 in evaluated case studies

| Case Studies | G2V [kWh] | V2V_inc [kWh] | V2V_out [kWh] | PV2V [kWh] | V2G [kWh] | Final SoE [kWh] | Desired SoE [kWh] | Comfort Violation [%] |
|---|---|---|---|---|---|---|---|---|
| Base Case -1 | 7.728 | - | - | - | - | 46.15 | 46.15 | 0 |
| Base Case -2 | 7.728 | - | - | - | - | 46.15 | 46.15 | 0 |
| Case 1 | 0 | - | - | - | 0 | 38.81 | 46.15 | 9.27 |
| Case 2 | 0 | - | - | - | 0 | 38.81 | 46.15 | 9.27 |
| Case 3 | 0 | 7.728 | 0 | - | 0 | 46.15 | 46.15 | 0 |
| Case 4 | 0 | 8.744 | 0.916 | - | 0 | 46.15 | 46.15 | 0 |
| Case 5 | 0 | - | - | 5.391 | 0 | 43.93 | 46.15 | 2.80 |
| Case 6 | 0 | - | - | 4.675 | 0 | 43.25 | 46.15 | 3.66 |
| Case 7 | 0 | 7.728 | 0 | 0 | 0 | 46.15 | 46.15 | 0 |
| Case 8 | 0 | 5.695 | 0 | 2.033 | 0 | 46.15 | 46.15 | 0 |

Table 4.7 summarizes the results for the EV-103 that is parked in the EVPL. In cases which the V2V operation is not active, disturbance of comfort in the EV is observed. Although the comfort violation is reduced with the help of PV, V2V transaction is necessary for comfort enhancement. The most power drawn from other EVs by V2V operation among the case studies is *Case-4*.

### 4.4.3 SoE and Power Variations of the EV - 28

In this subsection, the power and energy variations of an EV that is present in the EVPL between 8:15 am and 12:15 am and whose energy demand is 21.15 kWh are shown.

Figure 4.24 illustrates the power and energy state changes of the EV-28 in *Base Case-1* and *Base Case-2*. In *Base Case-1*, the EV begins charging immediately upon arrival at the EVPL, whereas in *Base Case-2*, the EV's charging process is delayed to the departure time due to the PLL operation. The EVPL's flexibility increases as the EV parking time increases.

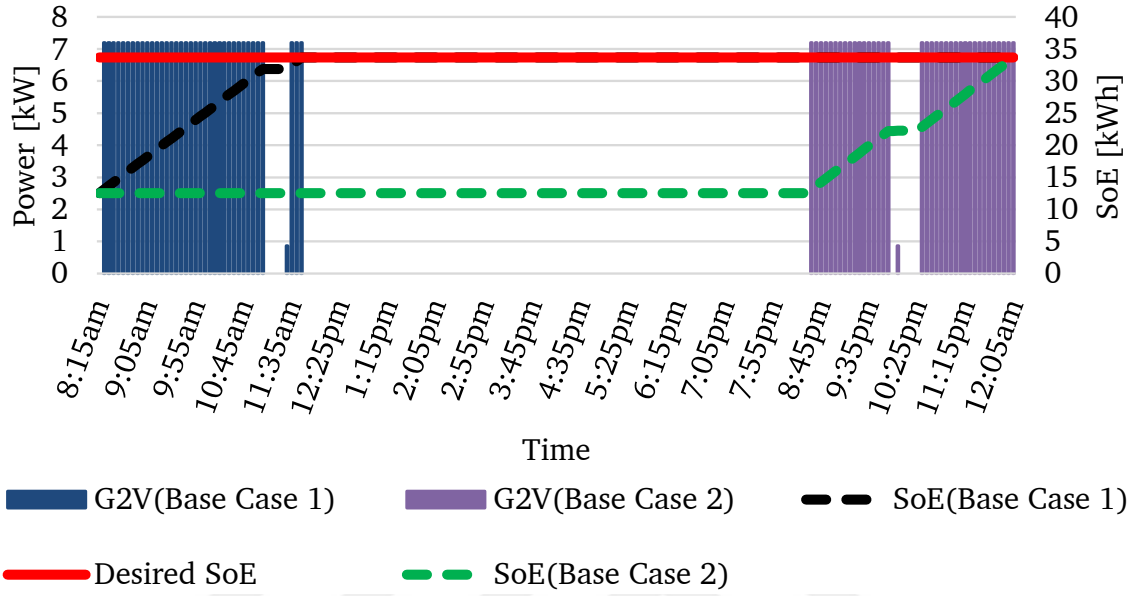



**Figure 4.24** SoE and power variations of EV-28 (Base Case-1 and Base Case-2)

Figure 4.25 illustrates the power and energy state changes of an EV with a long parking time in *Case-8*, which includes active V2V, V2G, PLL, and PV generation.When necessary, the EV-28 participates in V2V and V2G operations, assisting EVPL in operating optimally and enhancing EV comfort.

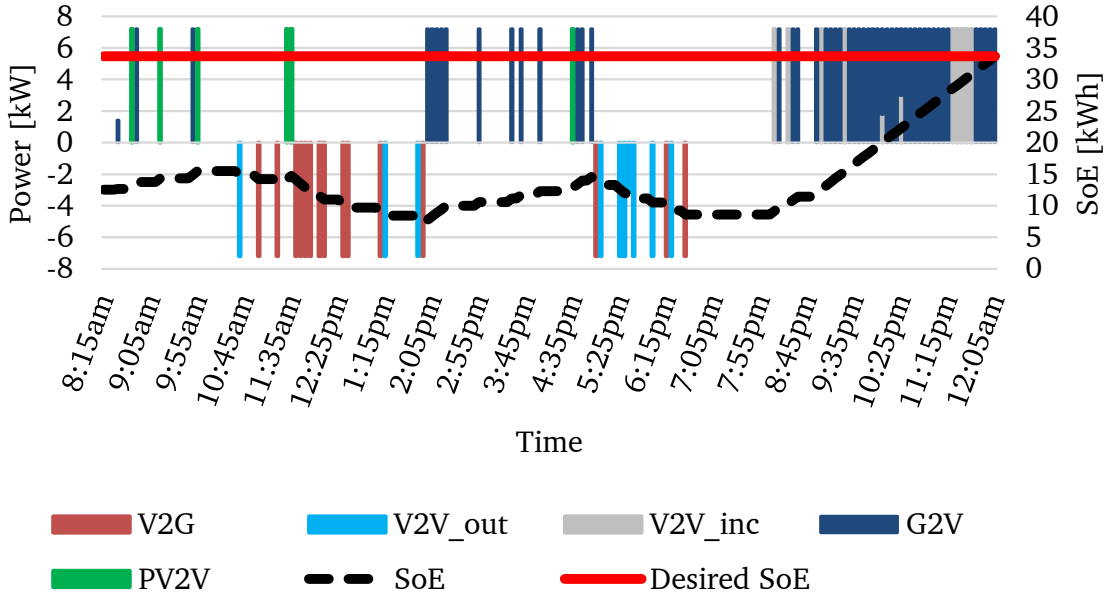



**Figure 4.25** SoE and power variations of EV-28 (Case-8)

Table 4.8 summarizes the results for the EV-28 that is parked in the EVPL. Despite the fact that the EVLP participates in V2V and V2G transactions, the EV's comfort is not violated in none of the case studies. However, despite the fact that it decreases with PV production, the high battery discharge should be examined further in terms of battery health.

**Table 4.8** Comparison of the results of EV-28 in evaluated case studies

| Case Studies | G2V [kWh] | V2V_inc [kWh] | V2V_out [kWh] | PV2V [kWh] | V2G [kWh] | Final SoE [kWh] | Desired SoE [kWh] | Comfort Violation [%] |
|---|---|---|---|---|---|---|---|---|
| Base Case -1 | 22.363 | - | - | - | - | 33.68 | 33.68 | 0 |
| Base Case -2 | 22.363 | - | - | - | - | 33.68 | 33.68 | 0 |
| Case 1 | 48.845 | - | - | - | 23.99 | 33.68 | 33.68 | 0 |
| Case 2 | 49.135 | - | - | - | 24.252 | 33.68 | 33.68 | 0 |
| Case 3 | 41.983 | 9.097 | 14.612 | - | 11.395 | 33.68 | 33.68 | 0 |
| Case 4 | 44.982 | 7.797 | 9.548 | - | 17.993 | 33.68 | 33.68 | 0 |
| Case 5 | 32.114 | - | - | 0.599 | 9.432 | 33.68 | 33.68 | 0 |
| Case 6 | 33.587 | - | - | 1.303 | 11.395 | 33.68 | 33.68 | 0 |
| Case 7 | 27.426 | 6.123 | 5.998 | 7.986 | 11.395 | 33.68 | 33.68 | 0 |
| Case 8 | 29.107 | 5.797 | 5.659 | 3.599 | 8.996 | 33.68 | 33.68 | 0 |

# 5
# RESULTS AND DISCUSSION

Electrical energy is a critical component of our civilization's development. Humanity has been advancing at a breakneck pace as a result of rapid industrialization. Global warming has become one of humanity's most serious problems as a result of the increase in GHG emissions caused by fossil fuels. Countries and companies are investing in green energy as the current order will not be sustainable for our world. Renewable energy sources and EVs will inevitably play a significant role in green energy and zero-carbon policies. As a result, the optimal integration of EVs and PVs into electrical power systems, while taking DR programs into account, is a critical research topic for sustainable energy management. Unlike conventional loads, EV batteries can be used as additional storage units in the balancing market via the V2X concept in the event of RES, load, or generation deficits.

Firstly, this thesis examined the comfort violation experienced by EVs participating in V2G and PLL operations in an EVPL equipped with PV. Following that, the effect of V2V transaction on comfort violation was evaluated using ten different case studies. Uncertainties in PV generation and the arrival time of EVs in EVPL were accounted with high accuracy rates for through the use of a machine learning approach based on LSTM cells, a special type of RNN.

The results of the applied case studies are summarized as follows:

- *Case-1* and *Case-2* both had the highest level of comfort violation of 4.82. Although the comfort violation decreased in *Case-5* and *Case-6* due to the activation of PV production compared to *Case-1* and *Case-2*, it was insufficient. In all cases containing V2V, a violation of the minimum level of comfort was observed. When the effect of PLL on comfort violation was examined, it was discovered that when compared to cases without PLL, PLL had no effect on average comfort violation.

- It has been observed EVPL draws the most energy from the grid in *Case-3* and *Case-4*, which contain V2V operation. It was seen that EVPL draws 4138.720 and 4132.639 kWh of energy in *Base Case-1* and *Base Case-2*, respectively, while the amount of energy consumed in *Case-3* and *Case-4* increases by almost %50 and draws 6037.188 and 6011.110 kWh, respectively. As a result, the system operator and EVPL manager must account for the increased grid power demand caused by V2V operation. On the other hand, it has been seen that PV is quite effective in reducing the power drawn from the grid. In contrast to the increase in *Case-3* and *Case-4*, there is only a %13 increase in energy drawn from the grid compared to *Base Case-1* and *Base Case-2*.

- Considering the load factor, it was seen that the load factor is less in all cases with PLL than in cases without. The lowest load factor is seen in *Case-2* with %17.68. Since it was not possible to draw power from the grid due to V2G and PLL, new peaks occurred and the load factor decreased. Additionally, the EVPL manager must account for any new peaks introduced by the PLL.

- V2V operation occur the most in *Case-4* with 1816.052 kWh. Compared to *Case-4*, in *Case-3*, it was seen that PLL caused 92.165 kWh more V2V energy exchange. In *Case-8*, on the other hand, thanks to the PV process, the PLL did not cause an increase in V2V or even a decrease of 29.918 kWh.

- In order to see the effect of the proposed model on EVs more clearly, the power and energy changes of 3 out of 253 EVs charged in EVPL were examined. When the results were analyzed in terms of EV comfort, it was seen that the V2V process significantly reduced/eliminated the comfort violation in EVs whose comfort was disturbed by V2G and PLL. In fact, it has been observed that EVs with increased comfort thanks to V2V, participate in the V2V process to increase the comfort of other EVs when necessary. However, when the results were analyzed in terms of an EV parked all day in the EVPL, it was discovered that the EV was charged and discharged multiple times throughout the day. As a result, the battery aging of EVs must also be considered.

As a result, with this thesis, it has been seen that the comfort violation of the EVs in an EVPL participating in the ancillary services to the grid in terms of the reduced energy that cannot be met due to these services is reduced with the help of V2V transaction. Moreover, the proposed model revealed that the V2X concept working together with PV is beneficial for the EVPL load profile. Within the scope of the future study, it is planned to develop the proposed model taking into account the decision-making mechanism of the DSO and to process the decision-making mechanism of the distribution system together with EVPL.

# REFERENCES


[1] IEA, "Global energy review 2020," 2020. DOI: 10.1787/a60abbf2-en.

[2] K. Steininger, M. König, B. Bednar-Friedl, W. Loibl, L. Kranzl, F. Prettenthaler, W. Haas, H. Formayer, M. Goetzl, K. Zulka, *Economic Evaluation of Climate Change Impacts - Development of a Cross-Sectoral Framework and Results for Austria*. Apr. 2015, ISBN: 978-3-319-12456-8. DOI: 10.1007/978-3-319-12457-5.

[3] IEA, *Global EV Outlook 2021*. 2021. [Online]. Available: https://www.iea.org/reports/global-ev-outlook-2021 (visited on ).

[4] D. Saygın, O. B. Tör, S. Teimourzadeh, M. Koç, J. Hildermeier, C. Kolokathis, *Transport sector transformation: Integrating electric vehicles into Turkey's distribution grids*. 2019.

[5] M. R. Khalid, M. S. Alam, A. Sarwar, M. Jamil Asghar, "A comprehensive review on electric vehicles charging infrastructures and their impacts on power-quality of the utility grid," *eTransportation*, vol. 1, p. 100 006, 2019, ISSN: 2590-1168. DOI: 10.1016/j.etran.2019.100006.

[6] J. A. P. Lopes, F. J. Soares, P. M. R. Almeida, "Integration of electric vehicles in the electric power system," *Proceedings of the IEEE*, vol. 99, no. 1, pp. 168–183, 2011. DOI: 10.1109/JPROC.2010.2066250.

[7] M. Ş. Kuran, A. Carneiro Viana, L. Iannone, D. Kofman, G. Mermoud, J. P. Vasseur, "A smart parking lot management system for scheduling the recharging of electric vehicles," *IEEE Transactions on Smart Grid*, vol. 6, no. 6, pp. 2942–2953, 2015. DOI: 10.1109/TSG.2015.2403287.

[8] E. Akhavan-Rezai, M. F. Shaaban, E. F. El-Saadany, F. Karray, "Online intelligent demand management of plug-in electric vehicles in future smart parking lots," *IEEE Systems Journal*, vol. 10, no. 2, pp. 483–494, 2016. DOI: 10.1109/JSYST.2014.2349357.

[9] İ. Şengör, O. Erdinç, B. Yener, A. Taşcıkaraoğlu, J. P. S. Catalão, "Optimal energy management of ev parking lots under peak load reduction based dr programs considering uncertainty," *IEEE Transactions on Sustainable Energy*, vol. 10, no. 3, pp. 1034–1043, 2019. DOI: 10.1109/TSTE.2018.2859186.

[10] İ. Şengör, S. Güner, O. Erdinç, "Real-time algorithm based intelligent ev parking lot charging management strategy providing pll type demand response program," *IEEE Transactions on Sustainable Energy*, vol. 12, no. 2, pp. 1256–1264, 2021. DOI: 10.1109/TSTE.2020.3040818.

[11] H. Zhang, Z. Hu, Z. Xu, Y. Song, "Optimal planning of pev charging station with single output multiple cables charging spots," *IEEE Transactions on Smart Grid*, vol. 8, no. 5, pp. 2119–2128, 2017. DOI: 10.1109/TSG.2016.2517026.

[12] W. Jiang, Y. Zhen, "A real-time ev charging scheduling for parking lots with pv system and energy store system," *IEEE Access*, vol. 7, pp. 86 184–86 193, 2019. DOI: 10.1109/ACCESS.2019.2925559.

[13] L. Zhang, Y. Li, "Optimal management for parking-lot electric vehicle charging by two-stage approximate dynamic programming," *IEEE Transactions on Smart Grid*, vol. 8, no. 4, pp. 1722–1730, 2017. DOI: 10.1109/TSG.2015.2505298.

[14] H. Chen, Z. Hu, H. Luo, J. Qin, R. Rajagopal, H. Zhang, "Design and planning of a multiple-charger multiple-port charging system for pev charging station," *IEEE Transactions on Smart Grid*, vol. 10, no. 1, pp. 173–183, 2019. DOI: 10.1109/TSG.2017.2735636.

[15] Y. Zhang, L. Cai, "Dynamic charging scheduling for ev parking lots with photovoltaic power system," *IEEE Access*, vol. 6, pp. 56 995–57 005, 2018. DOI: 10.1109/ACCESS.2018.2873286.

[16] A. S. A. Awad, M. F. Shaaban, T. H. M. EL-Fouly, E. F. El-Saadany, M. M. A. Salama, "Optimal resource allocation and charging prices for benefit maximization in smart pev-parking lots," *IEEE Transactions on Sustainable Energy*, vol. 8, no. 3, pp. 906–915, 2017. DOI: 10.1109/TSTE.2016.2617679.

[17] "Optimal performance of electric vehicles parking lot considering environmental issue," *Journal of Cleaner Production*, vol. 206, pp. 1073–1088, 2019, ISSN: 0959-6526. DOI: 10.1016/j.jclepro.2018.09.222.

[18] O. Fallah-Mehrjardi, M. H. Yaghmaee, A. Leon-Garcia, "Charge scheduling of electric vehicles in smart parking-lot under future demands uncertainty," *IEEE Transactions on Smart Grid*, vol. 11, no. 6, pp. 4949–4959, 2020. DOI: 10.1109/TSG.2020.3000850.

[19] M. Rahmani-Andebili, H. Shen, M. Fotuhi-Firuzabad, "Planning and operation of parking lots considering system, traffic, and drivers behavioral model," *IEEE Transactions on Systems, Man, and Cybernetics: Systems*, vol. 49, no. 9, pp. 1879–1892, 2019. DOI: 10.1109/TSMC.2018.2824122.

[20] B. Zeng, J. Feng, N. Liu, Y. Liu, "Co-optimized parking lot placement and incentive design for promoting pev integration considering decision-dependent uncertainties," *IEEE Transactions on Industrial Informatics*, vol. 17, no. 3, pp. 1863–1872, 2021. DOI: 10.1109/TII.2020.2993815.

[21] R. Xie, W. Wei, Q. Wu, T. Ding, S. Mei, "Optimal service pricing and charging scheduling of an electric vehicle sharing system," *IEEE Transactions on Vehicular Technology*, vol. 69, no. 1, pp. 78–89, 2020. DOI: 10.1109/TVT.2019.2950402.

[22] Y. Li, B. Hu, "A consortium blockchain-enabled secure and privacy-preserving optimized charging and discharging trading scheme for electric vehicles," *IEEE Transactions on Industrial Informatics*, vol. 17, no. 3, pp. 1968–1977, 2021. DOI: 10.1109/TII.2020.2990732.

[23] M. Moradijoz, M. Parsa Moghaddam, M.-R. Haghifam, "A flexible distribution system expansion planning model: A dynamic bi-level approach," *IEEE Transactions on Smart Grid*, vol. 9, no. 6, pp. 5867–5877, 2018. DOI: 10.1109/TSG.2017.2697917.

[24] M. J. Mirzaei, A. Kazemi, O. Homaee, "A probabilistic approach to determine optimal capacity and location of electric vehicles parking lots in distribution networks," *IEEE Transactions on Industrial Informatics*, vol. 12, no. 5, pp. 1963–1972, 2016. DOI: 10.1109/TII.2015.2482919.

[25] N. Neyestani, M. Y. Damavandi, M. Shafie-Khah, J. Contreras, J. P. S. Catalão, "Allocation of plug-in vehicles' parking lots in distribution systems considering network-constrained objectives," *IEEE Transactions on Power Systems*, vol. 30, no. 5, pp. 2643–2656, 2015. DOI: 10.1109/TPWRS.2014.2359919.

[26] M. Shafie-Khah, P. Siano, D. Z. Fitiwi, N. Mahmoudi, J. P. S. Catalão, "An innovative two-level model for electric vehicle parking lots in distribution systems with renewable energy," *IEEE Transactions on Smart Grid*, vol. 9, no. 2, pp. 1506–1520, 2018. DOI: 10.1109/TSG.2017.2715259.

[27] S. Deb, A. K. Goswami, P. Harsh, J. P. Sahoo, R. L. Chetri, R. Roy, A. S. Shekhawat, "Charging coordination of plug-in electric vehicle for congestion management in distribution system integrated with renewable energy sources," *IEEE Transactions on Industry Applications*, vol. 56, no. 5, pp. 5452–5462, 2020. DOI: 10.1109/TIA.2020.3010897.

[28] B. Zeng, Z. Zhu, H. Xu, H. Dong, "Optimal public parking lot allocation and management for efficient pev accommodation in distribution systems," *IEEE Transactions on Industry Applications*, vol. 56, no. 5, pp. 5984–5994, 2020. DOI: 10.1109/TIA.2020.2986980.

[29] M. Yazdani-Damavandi, M. P. Moghaddam, M.-R. Haghifam, M. Shafie-khah, J. P. S. Catalão, "Modeling operational behavior of plug-in electric vehicles' parking lot in multienergy systems," *IEEE Transactions on Smart Grid*, vol. 7, no. 1, pp. 124–135, 2016. DOI: 10.1109/TSG.2015.2404892.

[30] N. Neyestani, M. Y. Damavandi, M. Shafie-khah, A. G. Bakirtzis, J. P. S. Catalão, "Plug-in electric vehicles parking lot equilibria with energy and reserve markets," *IEEE Transactions on Power Systems*, vol. 32, no. 3, pp. 2001–2016, 2017. DOI: 10.1109/TPWRS.2016.2609416.

[31] J. Singh, R. Tiwari, "Cost benefit analysis for v2g implementation of electric vehicles in distribution system," *IEEE Transactions on Industry Applications*, vol. 56, no. 5, pp. 5963–5973, 2020. DOI: 10.1109/TIA.2020.2986185.

[32] Y. Huang, "Day-ahead optimal control of pev battery storage devices taking into account the voltage regulation of the residential power grid," *IEEE Transactions on Power Systems*, vol. 34, no. 6, pp. 4154–4167, 2019. DOI: 10.1109/TPWRS.2019.2917009.

[33] A. Tavakoli, M. Negnevitsky, S. Saha, M. E. Haque, M. T. Arif, J. Contreras, A. Oo, "Self-scheduling of a generating company with an ev load aggregator under an energy exchange strategy," *IEEE Transactions on Smart Grid*, vol. 10, no. 4, pp. 4253–4264, 2019. DOI: 10.1109/TSG.2018.2854763.

[34] S. Huang, Q. Wu, "Dynamic tariff-subsidy method for pv and v2g congestion management in distribution networks," *IEEE Transactions on Smart Grid*, vol. 10, no. 5, pp. 5851–5860, 2019. DOI: 10.1109/TSG.2019.2892302.

[35] S. M. B. Sadati, J. Moshtagh, M. Shafie-khah, A. Rastgou, J. P. Catalão, "Bi-level model for operational scheduling of a distribution company that supplies electric vehicle parking lots," *Electric Power Systems Research*, vol. 174, p. 105 875, 2019, ISSN: 0378-7796. DOI: 10.1016/j.epsr.2019.105875.

[36] P. Salyani, M. Abapour, K. Zare, "Stackelberg based optimal planning of dgs and electric vehicle parking lot by implementing demand response program," *Sustainable Cities and Society*, vol. 51, p. 101 743, 2019, ISSN: 2210-6707. DOI: 10.1016/j.scs.2019.101743.

[37] M. Vosoogh, M. Rashidinejad, A. Abdollahi, M. Ghaseminezhad, "An intelligent day ahead energy management framework for networked microgrids considering high penetration of electric vehicles," *IEEE Transactions on Industrial Informatics*, vol. 17, no. 1, pp. 667–677, 2021. DOI: 10.1109/TII.2020.2977989.

[38] M. Ebrahimi, M. Rastegar, M. Mohammadi, A. Palomino, M. Parvania, "Stochastic charging optimization of v2g-capable pevs: A comprehensive model for battery aging and customer service quality," *IEEE Transactions on Transportation Electrification*, vol. 6, no. 3, pp. 1026–1034, 2020. DOI: 10.1109/TTE.2020.3005875.

[39] N. Neyestani, M. Y. Damavandi, G. Chicco, J. P. S. Catalão, "Effects of pev traffic flows on the operation of parking lots and charging stations," *IEEE Transactions on Smart Grid*, vol. 9, no. 2, pp. 1521–1530, 2018. DOI: 10.1109/TSG.2017.2728368.

[40] H. S. V. S. K. Nunna, S. Battula, S. Doolla, D. Srinivasan, "Energy management in smart distribution systems with vehicle-to-grid integrated microgrids," *IEEE Transactions on Smart Grid*, vol. 9, no. 5, pp. 4004–4016, 2018. DOI: 10.1109/TSG.2016.2646779.

[41] X. Chen, K.-C. Leung, "Non-cooperative and cooperative optimization of scheduling with vehicle-to-grid regulation services," *IEEE Transactions on Vehicular Technology*, vol. 69, no. 1, pp. 114–130, 2020. DOI: 10.1109/TVT.2019.2952712.

[42] Maigha, M. L. Crow, "Electric vehicle scheduling considering co-optimized customer and system objectives," *IEEE Transactions on Sustainable Energy*, vol. 9, no. 1, pp. 410–419, 2018. DOI: 10.1109/TSTE.2017.2737146.

[43] G. R. Chandra Mouli, M. Kefayati, R. Baldick, P. Bauer, "Integrated pv charging of ev fleet based on energy prices, v2g, and offer of reserves," *IEEE Transactions on Smart Grid*, vol. 10, no. 2, pp. 1313–1325, 2019. DOI: 10.1109/TSG.2017.2763683.

[44] P. Sanchez-Martin, G. Sanchez, G. Morales-Espana, "Direct load control decision model for aggregated ev charging points," *IEEE Transactions on Power Systems*, vol. 27, no. 3, pp. 1577–1584, 2012. DOI: 10.1109/TPWRS.2011.2180546.

[45] M. Wang, M. Ismail, R. Zhang, X. S. Shen, E. Serpedin, K. Qaraqe, "A semi-distributed v2v fast charging strategy based on price control," in *2014 IEEE Global Communications Conference*, 2014, pp. 4550–4555. DOI: 10.1109/GLOCOM.2014.7037525.

[46] M. Wang, M. Ismail, R. Zhang, X. Shen, E. Serpedin, K. Qaraqe, "Spatio-temporal coordinated v2v energy swapping strategy for mobile pevs," *IEEE Transactions on Smart Grid*, vol. 9, no. 3, pp. 1566–1579, 2018. DOI: 10.1109/TSG.2016.2593667.

[47] P. You, Z. Yang, "Efficient optimal scheduling of charging station with multiple electric vehicles via v2v," in *2014 IEEE International Conference on Smart Grid Communications (SmartGridComm)*, 2014, pp. 716–721. DOI: 10.1109/SmartGridComm.2014.7007732.

[48] P. You, Z. Yang, M.-Y. Chow, Y. Sun, "Optimal cooperative charging strategy for a smart charging station of electric vehicles," *IEEE Transactions on Power Systems*, vol. 31, no. 4, pp. 2946–2956, 2016. DOI: 10.1109/TPWRS.2015.2477372.

[49] R. Alvaro, J. González, C. Gamallo, J. Fraile-Ardanuy, D. L. Knapen, "Vehicle to vehicle energy exchange in smart grid applications," in *2014 International Conference on Connected Vehicles and Expo (ICCVE)*, 2014, pp. 178–184. DOI: 10.1109/ICCVE.2014.7297538.

[50] A. M. Koufakis, E. S. Rigas, N. Bassiliades, S. D. Ramchurn, "Towards an optimal ev charging scheduling scheme with v2g and v2v energy transfer," in *2016 IEEE International Conference on Smart Grid Communications (SmartGridComm)*, 2016, pp. 302–307. DOI: 10.1109/SmartGridComm.2016.7778778.

[51] A. M. Koufakis, E. S. Rigas, N. Bassiliades, S. D. Ramchurn, "Offline and online electric vehicle charging scheduling with v2v energy transfer," *IEEE Transactions on Intelligent Transportation Systems*, vol. 21, no. 5, pp. 2128–2138, 2020. DOI: 10.1109/TITS.2019.2914087.

[52] J. Kang, R. Yu, X. Huang, S. Maharjan, Y. Zhang, E. Hossain, "Enabling localized peer-to-peer electricity trading among plug-in hybrid electric vehicles using consortium blockchains," *IEEE Transactions on Industrial Informatics*, vol. 13, no. 6, pp. 3154–3164, 2017. DOI: 10.1109/TII.2017.2709784.

[53] R. Zhang, X. Cheng, L. Yang, "Flexible energy management protocol for cooperative ev-to-ev charging," *IEEE Transactions on Intelligent Transportation Systems*, vol. 20, no. 1, pp. 172–184, 2019. DOI: 10.1109/TITS.2018.2807184.

[54] G. Li, Q. Sun, L. Boukhatem, J. Wu, J. Yang, "Intelligent vehicle-to-vehicle charging navigation for mobile electric vehicles via vanet-based communication," *IEEE Access*, vol. 7, pp. 170 888–170 906, 2019. DOI: 10.1109/ACCESS.2019.2955927.

[55] X. Huang, Y. Zhang, D. Li, L. Han, "An optimal scheduling algorithm for hybrid ev charging scenario using consortium blockchains," *Future Generation Computer Systems*, vol. 91, pp. 555–562, 2019. DOI: 10.1016/j.future.2018.09.046.

[56] L. Zeng, C. Li, Z. Li, M. Shahidehpour, B. Zhou, Q. Zhou, "Hierarchical bipartite graph matching method for transactive v2v power exchange in distribution power system," *IEEE Transactions on Smart Grid*, vol. 12, no. 1, pp. 301–311, 2021. DOI: 10.1109/TSG.2020.3016597.

[57] P. J. Chacko, M. Sachidanandam, "An optimized energy management system for vehicle to vehicle power transfer using micro grid charging station integrated gridable electric vehicles," *Sustainable Energy, Grids and Networks*, vol. 26, p. 100 474, 2021. DOI: 10.1016/j.segan.2021.100474.

[58] A. Al-Obaidi, H. Khani, H. E. Farag, M. Mohamed, "Bidirectional smart charging of electric vehicles considering user preferences, peer to peer energy trade, and provision of grid ancillary services," *International Journal of Electrical Power Energy Systems*, vol. 124, p. 106 353, 2021. DOI: 10.1016/j.ijepes.2020.106353.

[59] M. Mozaffari, H. Askarian Abyaneh, M. Jooshaki, M. Moeini-Aghtaie, "Joint expansion planning studies of ev parking lots placement and distribution network," *IEEE Transactions on Industrial Informatics*, vol. 16, no. 10, pp. 6455–6465, 2020. DOI: 10.1109/TII.2020.2964049.

[60] C. Liu, K. T. Chau, D. Wu, S. Gao, "Opportunities and challenges of vehicle-to-home, vehicle-to-vehicle, and vehicle-to-grid technologies," *Proceedings of the IEEE*, vol. 101, no. 11, pp. 2409–2427, 2013. DOI: 10.1109/JPROC.2013.2271951.

[61] N. Bañol Arias, S. Hashemi, P. B. Andersen, C. Træholt, R. Romero, "Distribution system services provided by electric vehicles: Recent status, challenges, and future prospects," *IEEE Transactions on Intelligent Transportation Systems*, vol. 20, no. 12, pp. 4277–4296, 2019. DOI: 10.1109/TITS.2018.2889439.

[62] *V2g around the world*, https://www.v2g-hub.com/, [Online; accessed 01-June-2021].

[63] K. M. Tan, V. K. Ramachandaramurthy, J. Y. Yong, "Integration of electric vehicles in smart grid: A review on vehicle to grid technologies and optimization techniques," *Renewable and Sustainable Energy Reviews*, vol. 53, pp. 720–732, 2016, ISSN: 1364-0321. DOI: 10.1016/j.rser.2015.09.012.

[64] *Understanding lstm networks*, https://colah.github.io/posts/2015-08-Understanding-LSTMs/, [Online; accessed 01-June-2021].

[65] M. Phi, *Illustrated guide to lstm's and gru's: A step by step explanation*, https://towardsdatascience.com/illustrated-guide-to-lstms-and-gru-s-a-step-by-step-explanation-44e9eb85bf21, [Online; accessed 01-June-2021], Jun. 2020.

[66] A. Ng, *Long short term memory (lstm) - recurrent neural networks*, https://www.coursera.org/lecture/nlp-sequence-models/long-short-term-memory-lstm-KXoay?utm_source=link&utm_medium=page_share&utm_content=in_course_lecture&utm_campaign=bar_button, [Online; accessed 01-June-2021].

[67] H. G. Santos, T. A. Toffolo, "Mixed integer linear programming with python," 2020.

[68] L. Gurobi Optimization, *Gurobi optimizer reference manual*, http://www.gurobi.com, [Online; accessed 01-June-2021], 2021.

[69] E.. Bisong, *Building Machine Learning and Deep Learning Models on Google Cloud Platform A Comprehensive Guide for Beginners*. Apress, 2019.

[70] S. Hochreiter, J. Schmidhuber, "Long short-term memory," *Neural Computation*, vol. 9, no. 8, pp. 1735–1780, Nov. 1997, ISSN: 0899-7667. DOI: 10.1162/neco.1997.9.8.1735.

[71] S. Guner, A. Ozdemir, "Reliability improvement of distribution system considering EV parking lots," *Electric Power Systems Research*, vol. 185, p. 106 353, 2020, ISSN: 0378-7796. DOI: 10.1016/j.epsr.2020.106353.

[72] D. Jager, A. Andreas, "Nrel national wind technology center (nwtc): M2 tower; boulder, colorado (data); nrel report no. da-5500-56489," 1996. DOI: 10.5439/1052222.

[73] M. Abadi, A. Agarwal, P. Barham, E. Brevdo, Z. Chen, C. Citro, G. S. Corrado, A. Davis, J. Dean, M. Devin, S. Ghemawat, I. Goodfellow, A. Harp, G. Irving, M. Isard, Y. Jia, R. Jozefowicz, L. Kaiser, M. Kudlur, J. Levenberg, D. Mané, R. Monga, S. Moore, D. Murray, C. Olah, M. Schuster, J. Shlens, B. Steiner, I. Sutskever, K. Talwar, P. Tucker, V. Vanhoucke, V. Vasudevan, F. Viégas, O. Vinyals, P. Warden, M. Wattenberg, M. Wicke, Y. Yu, X. Zheng, *TensorFlow: Large-scale machine learning on heterogeneous systems*, Software available from tensorflow.org, 2015.

[74] F. Chollet *et al.*, *Keras*, https://keras.io, 2015.

[75] P. Virtanen, R. Gommers, T. E. Oliphant, M. Haberland, T. Reddy, D. Cournapeau, E. Burovski, P. Peterson, W. Weckesser, J. Bright, S. J. van der Walt, M. Brett, J. Wilson, K. J. Millman, N. Mayorov, A. R. J. Nelson, E. Jones, R. Kern, E. Larson, C. J. Carey, İ. Polat, Y. Feng, E. W. Moore, J. VanderPlas, D. Laxalde, J. Perktold, R. Cimrman, I. Henriksen, E. A. Quintero, C. R. Harris, A. M. Archibald, A. H. Ribeiro, F. Pedregosa, P. van Mulbregt, SciPy 1.0 Contributors, "SciPy 1.0: Fundamental Algorithms for Scientific Computing in Python," *Nature Methods*, vol. 17, pp. 261–272, 2020. DOI: 10.1038/s41592-019-0686-2.

[76] W. McKinney, "Data Structures for Statistical Computing in Python," in *Proceedings of the 9th Python in Science Conference*, S. van der Walt, J. Millman, Eds., 2010, pp. 56–61. DOI: 10.25080/Majora-92bf1922-00a.

[77] T. pandas development team, *Pandas-dev/pandas: Pandas*, version latest, Feb. 2020. DOI: 10.5281/zenodo.3509134. [Online]. Available: 10.5281/zenodo.3509134.

[78] *2020 Audi e-tron Sportback 55 quattro - Specifications*. https://www.evspecifications.com/en/model/4fcef4, [Online; accessed 04-December-2020].

[79] *2020 BMW i3s Edition RoadStyle 42 kWh - Specifications*. https://www.evspecifications.com/en/model/dcc6cf, [Online; accessed 04-December-2020].

[80] *2020 Tesla Model X Performance (PMSR) - Specifications*. https://www.evspecifications.com/en/model/2d24e4, [Online; accessed 04-December-2020].

[81] *2020 Chevrolet Bolt EV - Specifications*. https://www.evspecifications.com/en/model/0545d6, [Online; accessed 04- December-2020].

[82] *2020 Mercedes-Benz EQC 400 4MATIC - Specifications.* https://www.evspecifications.com/en/model/c7d2a8, [Online; accessed 04-December-2020].

[83] *2019 Hyundai KONA Electric 39 kWh - Specifications.* https://www.evspecifications.com/en/model/42546b, [Online; accessed 04-December-2020].

[84] *2020 Volkswagen e-Golf SE - Specifications.* https://www.evspecifications.com/en/model/7d1ddc, [Online; accessed 04-December-2020].

[85] *2020 KIA Soul EV 39 kWh - Specifications.* https://www.evspecifications.com/en/model/f5ffa1, [Online; accessed 04-December-2020].

[86] *2020 Porsche Taycan 4S - Specifications.* https://www.evspecifications.com/en/model/0c44ce, [Online; accessed 04- December-2020].

[87] *2020 SEAT Mii electric - Specifications.* https://www.evspecifications.com/en/model/cb4ffc, [Online; accessed 04- December-2020].

# A
# PYTHON CODES

## A.1 Python Codes for Base Case-1, Base Case-2, Case-1, Case-2, Case-5 and Case 6

```
# Import related libraries
from mip import
from itertools import product
from data import

#Create optimization model
m = Model(sense=MINIMIZE, solver_name=GRB)

#Define all variables
SOE = [[m.add_var('SOE({},{})'.format(n,t)) for t in T] for n in N]
P_ev_ch =[[m.add_var('P_ev_ch({},{})'.format(n,t),lb=0,ub=CR[n])
    for t in T] for n in N]
P_ev_dsch = [[m.add_var('P_ev_dsch({},{})'.format(n,t),lb=0,ub=CR[n
    ]) for t in T] for n in N]
P_V2G =[[m.add_var('P_V2G({},{})'.format(n,t),lb=0) for t in T] for
     n in N]
P_PV2V =[[m.add_var('P_PV2V({},{})'.format(n,t),lb=0) for t in T]
    for n in N]
P_PV_tot = [m.add_var('P_PV_tot({})'.format(t),lb=0) for t in T]
P_G2V = [[m.add_var('P_G2V({},{})'.format(n,t),lb=0) for t in T]
    for n in N]
P_V2G_tot = [m.add_var('P_V2G_tot({})'.format(t),lb=0) for t in T]
P_G2V_tot = [m.add_var('P_G2V_tot({})'.format(t),lb=0,ub=1000) for
    t in T] # ub = Limit[t] if PLL operations is active.
u1 = [[m.add_var('u1({},{})'.format(n,t), var_type=BINARY) for t in
     T] for n in N]
u2 =[m.add_var('u2({})'.format(t),var_type=BINARY) for t in T]
u3 = [m.add_var('u3({})'.format(n),var_type=BINARY) for n in N]
SOE_final = [m.add_var('SOE_final({})'.format(n),lb=0) for n in N]
SOE_n = [m.add_var('SOE_n({})'.format(n),lb=0) for n in N]
SOE_p = [m.add_var('SOE_p({})'.format(n),lb=0) for n in N]
VIO = [m.add_var('VIO({})'.format(n),lb=0) for n in N]
```

```
#Define equations and constraints of EVs
for (n,t) in product(N,T):
    if Ta[n] < t <= Td[n]:
        m += SOE[n][t] >= soe_min[n]
        m += SOE[n][t] <= BatCap[n]
        m += P_ev_dsch[n][t] == P_V2G[n][t]
        m += P_ev_ch[n][t] == P_G2V[n][t] + P_PV2V[n][t]
        m += P_ev_ch[n][t] <= CR[n] x u1[n][t]
        m += P_ev_dsch[n][t] <= CR[n] x (1 - u1[n][t])
        if t-1 == Ta[n]:
            m += SOE[n][t] == SOE_init_04[n] + (CE[n]xP_ev_ch[n][t]
   xDT) - (P_ev_dsch[n][t] x DT / CE[n])
        elif Ta[n] < t < Td[n]:
            m += SOE[n][t] == SOE[n][t-1] + (CE[n]xP_ev_ch[n][t]xDT
   ) - (P_ev_dsch[n][t] x DT / CE[n])
        elif t == Td[n]:
            m += SOE[n][t] == SOE[n][t - 1] + (CE[n] x P_ev_ch[n][t
   ] x DT) - (P_ev_dsch[n][t] x DT / CE[n])
            m += SOE[n][t] >= SOE_init_04[n]
            m += SOE_final[n] == SOE[n][t]
            m += SOE[n][t] <= soe_des_04[n]
    elif t == Ta[n]:
        m += SOE[n][t] == SOE_init_04[n]
        m += P_ev_dsch[n][t] == 0
        m += P_ev_ch[n][t] == 0
        m += P_V2G[n][t] == 0
        m += P_G2V[n][t] == 0
        m += P_PV2V[n][t] == 0
    else:
        m += SOE[n][t] == 0
        m += P_ev_dsch[n][t] == 0
        m += P_ev_ch[n][t] == 0
        m += P_V2G[n][t] == 0
        m += P_G2V[n][t] == 0
        m += P_PV2V[n][t] == 0

#Define equations and constraints of EVPL

for t in T:
    m += P_V2G_tot[t] == xsum(P_V2G[n][t] for n in N)
    m += P_G2V_tot[t] == xsum(P_G2V[n][t] for n in N)
    m += P_V2G_tot[t] == PGR_contract[t] # In Base Case-1, Base
   Case-2, Case-1 and Case-3 PGR_contract[t]=0
    m += P_V2G_tot[t] <= Nn x u2[t]
    m += P_G2V_tot[t] <= Nn x (1 - u2[t])
    m += P_PV_tot[t] == xsum(P_PV2V[n][t] for n in N)
    m += P_PV_tot[t] == PV_production[t] # If PV generation is not
   active, PV_production[t]=0
```

```
#Calculate comfort violation for all EVs
for n in N:
    m += SOE_final[n] == soe_des_04[n] + SOE_p[n] - SOE_n[n]
    m += SOE_n[n] <= Nn x (1 - u3[n])
    m += SOE_p[n] <= Nn x u3[n]
    m += VIO[n] == SOE_n[n] x 100 / BatCap[n]

#Define objective function
m.objective = xsum(VIO[n] for n in N) / len(BatCap)

#Solve optimization problem
m.max_gap = 0.00
status = m.optimize()

#Print results
if status == OptimizationStatus.OPTIMAL:
    print('optimal solution cost {} found'.format(m.objective_value
    ))

elif status == OptimizationStatus.FEASIBLE:
    print('sol.cost {} found, best possible: {}'.format(m.
    objective_value, m.objective_bound))

elif status == OptimizationStatus.NO_SOLUTION_FOUND:
    print('no feasible solution found, lower bound is: {}'.format(m
    .objective_bound))

if status == OptimizationStatus.OPTIMAL or status ==
    OptimizationStatus.FEASIBLE:
    print('solution:')
```

## A.2 Python Codes for Case-3, Case-4, Case-7 and Case-8

```
# Import related libraries
from mip import
from itertools import product
from data import

#Create optimization model
m = Model(sense=MINIMIZE, solver_name=GRB)

#Define all variables
SOE = [[m.add_var('SOE({},{})'.format(n,t)) for t in T] for n in N]
P_ev_ch =[[m.add_var('P_ev_ch({},{})'.format(n,t),lb=0,ub=CR[n])
    for t in T] for n in N]
P_ev_dsch = [[m.add_var('P_ev_dsch({},{})'.format(n,t),lb=0,ub=CR[n
    ]) for t in T] for n in N]
P_V2G =[[m.add_var('P_V2G({},{})'.format(n,t),lb=0) for t in T] for
     n in N]
P_PV2V =[[m.add_var('P_PV2V({},{})'.format(n,t),lb=0) for t in T]
    for n in N]
P_PV_tot = [m.add_var('P_PV_tot({})'.format(t),lb=0) for t in T]
P_V2V_out = [[m.add_var('P_V2V_out({},{})'.format(n,t),lb=0,ub=CR[n
    ]) for t in T] for n in N]
P_G2V = [[m.add_var('P_G2V({},{})'.format(n,t),lb=0) for t in T]
    for n in N] # ub = Limit[t] if PLL operations is active.
P_V2V_inc = [[m.add_var('P_V2V_inc({},{})'.format(n,t),lb=0,ub=CR[n
    ]) for t in T] for n in N]
P_V2G_tot = [m.add_var('P_V2G_tot({})'.format(t),lb=0) for t in T]
P_G2V_tot = [m.add_var('P_G2V_tot({})'.format(t),lb=0,ub=1000) for
    t in T]
u1 = [[m.add_var('u1({},{})'.format(n,t), var_type=BINARY) for t in
     T] for n in N]
u2 =[m.add_var('u2({})'.format(t),var_type=BINARY) for t in T]
u3 = [m.add_var('u3({})'.format(n),var_type=BINARY) for n in N]
SOE_final = [m.add_var('SOE_final({})'.format(n),lb=0) for n in N]
SOE_n = [m.add_var('SOE_n({})'.format(n),lb=0) for n in N]
SOE_p = [m.add_var('SOE_p({})'.format(n),lb=0) for n in N]
VIO = [m.add_var('VIO({})'.format(n),lb=0) for n in N]


#Define equations and constraints of EVs
for (n,t) in product(N,T):
    if Ta[n] < t <= Td[n]:
        m += SOE[n][t] >= soe_min[n]
        m += SOE[n][t] <= BatCap[n]
        m += P_ev_dsch[n][t] == P_V2G[n][t] + P_V2V_out[n][t]
        m += P_ev_ch[n][t] == P_G2V[n][t] + P_V2V_inc[n][t] +
   P_PV2V[n][t]
        m += P_ev_ch[n][t] <= CR[n] x u1[n][t]
        m += P_ev_dsch[n][t] <= CR[n] x (1 - u1[n][t])
```

```
        if t-1 == Ta[n]:
            m += SOE[n][t] == SOE_init_04[n] + (CE[n]xP_ev_ch[n][t]
    xDT) - (P_ev_dsch[n][t] x DT / CE[n])
        elif Ta[n] < t < Td[n]:
            m += SOE[n][t] == SOE[n][t-1] + (CE[n]xP_ev_ch[n][t]xDT
    ) - (P_ev_dsch[n][t] x DT / CE[n])
        elif t == Td[n]:
            m += SOE[n][t] == SOE[n][t - 1] + (CE[n] x P_ev_ch[n][t
    ] x DT) - (P_ev_dsch[n][t] x DT / CE[n])
            m += SOE[n][t] >= SOE_init_04[n]
            m += SOE_final[n] == SOE[n][t]
            m += SOE[n][t] <= soe_des_04[n]
     elif t == Ta[n]:
        m += SOE[n][t] == SOE_init_04[n]
        m += P_ev_dsch[n][t] == 0
        m += P_ev_ch[n][t] == 0
        m += P_V2V_out[n][t] == 0
        m += P_V2V_inc[n][t] == 0
        m += P_V2G[n][t] == 0
        m += P_G2V[n][t] == 0
        m += P_PV2V[n][t] == 0
     else:
        m += SOE[n][t] == 0
        m += P_ev_dsch[n][t] == 0
        m += P_ev_ch[n][t] == 0
        m += P_V2V_inc[n][t] == 0
        m += P_V2V_out[n][t] == 0
        m += P_V2G[n][t] == 0
        m += P_G2V[n][t] == 0
        m += P_PV2V[n][t] == 0

#Define equations and constraints of EVPL
for t in T:
    m += xsum(P_V2V_out[n][t] for n in N) == xsum(P_V2V_inc[n][t]
    for n in N)
    m += P_V2G_tot[t] == xsum(P_V2G[n][t] for n in N)
    m += P_G2V_tot[t] == xsum(P_G2V[n][t] for n in N)
    m += P_V2G_tot[t] == PGR_contract[t] # In Case-5 and Case-7
    PGR_contract[t]=0
    m += P_V2G_tot[t] <= Nn x u2[t]
    m += P_G2V_tot[t] <= Nn x (1 - u2[t])
    m += P_PV_tot[t] == xsum(P_PV2V[n][t] for n in N)
    m += P_PV_tot[t] == PV_production[t] # If PV generation is not
    active, PV_production[t]=0

#Calculate comfort violation for all EVs
for n in N:
    m += SOE_final[n] == soe_des_04[n] + SOE_p[n] - SOE_n[n]
    m += SOE_n[n] <= Nn x (1 - u3[n])
    m += SOE_p[n] <= Nn x u3[n]
    m += VIO[n] == SOE_n[n] x 100 / BatCap[n]
```

```
#Define objective function
m.objective = xsum(VIO[n] for n in N) / len(BatCap)

#Solve optimization problem
m.max_gap = 0.00
status = m.optimize()

#Print results
if status == OptimizationStatus.OPTIMAL:
    print('optimal solution cost {} found'.format(m.objective_value
    ))

elif status == OptimizationStatus.FEASIBLE:
    print('sol.cost {} found, best possible: {}'.format(m.
    objective_value, m.objective_bound))

elif status == OptimizationStatus.NO_SOLUTION_FOUND:
    print('no feasible solution found, lower bound is: {}'.format(m
    .objective_bound))

if status == OptimizationStatus.OPTIMAL or status ==
    OptimizationStatus.FEASIBLE:
    print('solution:')
```

# PUBLICATIONS FROM THE THESIS

## Conference Papers

1. H. C. Güldorum, İ. Şengör and O. Erdinç, "Charging Management System for Electric Vehicles considering Vehicle-to-Vehicle (V2V) Concept," 2020 12th International Conference on Electrical and Electronics Engineering (ELECO), 2020, pp. 188-192, doi: 10.1109/ELECO51834.2020.00050.